Spatial Scale of Agglomeration and Dispersion: Number, Spacing, and the Spatial Extent of Cities

Takashi Akamatsu
Tohoku Univ.

Tomoya Mori
Kyoto Univ., RIETI

Minoru Osawa
Kyoto Univ.

Yuki Takayama
Science Tokyo

February 27, 2026

How does transport cost affect the spatial organization of economic activities? This study develops a theoretical framework that distinguishes between two types of dispersion forces in spatial models: "local" dispersion forces acting *within* cities, and "global" dispersion forces acting *across* them. The distinction leads to a systematic classification of spatial models into a few fundamental types, each with distinct endogenous spatial patterns and comparative statics in response to changes in transport costs. The framework reconciles empirical findings and clarifies how transport-induced reorganization of economic activities can depend on the spatial scale of dominant dispersion forces.

JEL: C62, R12, R13
Keywords: agglomeration; spatial scale; quantitative spatial models.

*TA: akamatsu@plan.civil.tohoku.ac.jp, TM: mori@kier.kyoto-u.ac.jp, MO: osawa.minoru.4z@kyoto-u.ac.jp, YT: takayama.y.cc65@m.isct.ac.jp. We are deeply grateful to Co-Editor Gilles Duranton for his guidance and support throughout the review process, which enormously improved the paper. We also thank two thoughtful referees for very helpful comments. We thank Treb Allen, Kristian Behrens, Donald Davis, Yasusada Murata, Jonathan Newton, Michael Pflüger, Diego Puga, Esteban Rossi-Hansberg, Shunsuke Segi, Akihisa Shibata, and Jacques-François Thisse for their comments, including those for the earlier versions of this paper. We also thank all seminar and conference participants. This research has been supported by JSPS KAKENHI 17H00987, 18H01556, 19K15108, 21K04299, 22K04353, 23K22880, 23K22887, 24K00999, and 25H00543. This research was conducted as part of the project, "Agglomeration-based Framework for Empirical and Policy Analyses of Regional Economies," undertaken at the Research Institute of Economy, Trade and Industry. We acknowledge financial support from the Kajima Foundations and the Murata Science Foundation.

1 Introduction

Urban development often exhibits patterns that appear contradictory at first glance. In Japan, over the five decades from 1970 to 2020, urban populations became increasingly concentrated in larger cities. The share of the national population residing in the top 100 cities rose from 57% to 73%, while the share in the remaining cities fell from 8.7% to 7.1%, as reflected in the flatter slope of the rank–size plot (Fig. 1A). Concurrently, however, populations dispersed spatially within individual cities. The average city experienced a 35 % decline in its maximum population density and a 19 % decline in average density (Fig. 1B), a trend visible in the flattening of within-city distributions (e.g., Fig. 1C). The dual trend, economy-wide concentration coupled with intra-urban decentralization, is not unique to Japan but is observed across diverse contexts, including China, France, and the United States.[1]

How can population simultaneously concentrate across cities and spread out within them? Transport costs have been central to theories of economic agglomeration and dispersion. Indeed, Japan's spatial reorganization coincided with the rapid expansion of nationwide high-speed railway and highway networks, which were essentially developed from scratch between 1970 and 2020.[2] However, interpreting this dual pattern through existing theory is not straightforward. This is because most analyses consider highly stylized few-location settings, which makes it difficult to analyze how agglomeration and dispersion occur in complex spatial economies with many locations.

To address this, the present study develops a unified theoretical framework that distinguishes between "local" dispersion forces acting *within* cities and "global" dispersion forces acting *across* them. The core intuition is that dispersion, or the tendency for economic activity to spread out, operates at two distinct spatial scales: one pushing agents toward the fringes of their own city, and another repelling cities away from one another. This distinction clarifies how transport-induced reorganization depends on the dominant dispersion force.

To understand the core intuition, consider a hypothetical many-location economy with mobile agents, such as households or firms, making location choices. For exposition purposes, "locations" refer to generic discrete units such as regions, counties, cities, or grid cells. Suppose that agents benefit from proximity to others through some agglomeration forces. In the absence of dispersion forces, everyone concentrates in a single location, as illustrated by Fig. 2A.

[1] See Appendix B for detailed discussion. Combes et al. (2023) report similar evidence for France using newly constructed panel data spanning 1760–2020.

[2] Between 1970 and 2020, the total length increased from 1,119 km to 9,050 km for highways, and from 515 km to 3,106 km for high-speed railways. This is an increase of more than eight times and six times, respectively. See Fig. B.1 in Appendix B.

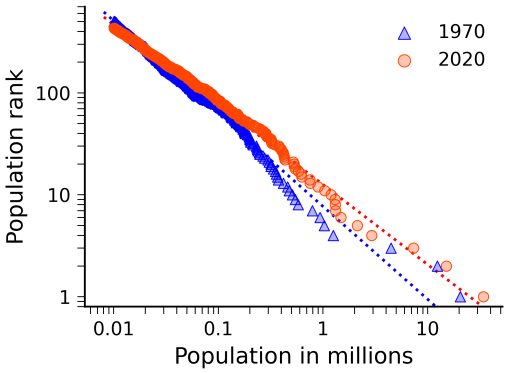

(A) Population rank–size plot

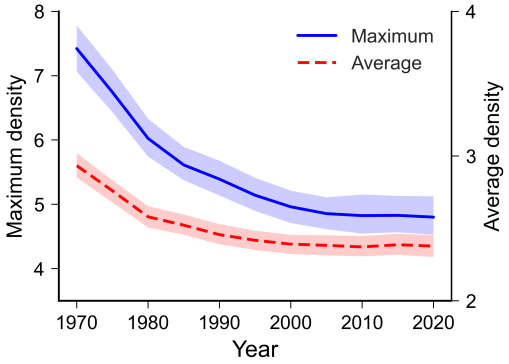

(B) Population density (1,000/km^2)

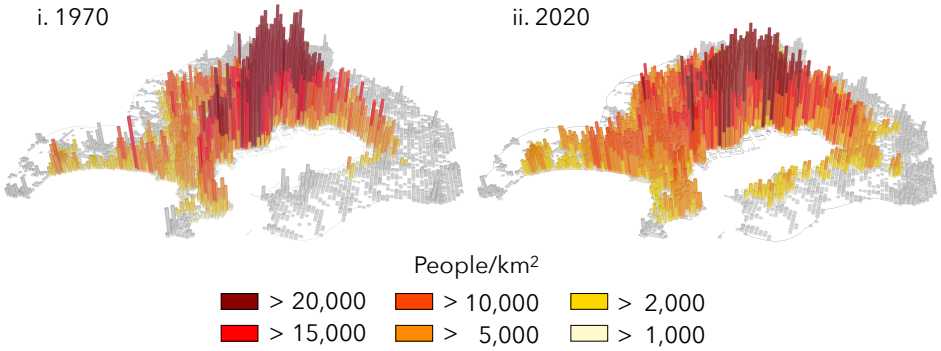

(C) The population distribution within Tokyo in 1970 (left) and 2020 (right)

Figure 1: Global concentration and local dispersion in Japan from 1970 to 2020.

Note: A *city* is defined as a cluster of contiguous 1km-by-1km grid cells, each with a population density of at least 1,000/km^2 and collectively comprising at least 10,000 residents. The number of cities decreased from 504 in 1970 to 431 in 2020. Panel (B) shows the annual cross-city arithmetic means of maximum and average population densities along with the 95% bootstrap confidence interval. Panel (C) shows the within-city population distribution in Tokyo in 1970 and 2020. For further discussion, see Appendix B. Reproduction data for the figures in this paper are available in Akamatsu et al. (2026).

First, consider the crowding effects that arise *within* a location, depend on its own population, and affect only its residents. We term such effects "local" dispersion forces. A representative example is crowding in the market for non-tradable goods. For instance, if the housing supply is inelastic, population growth within a location drives up housing prices, creating incentives for residents to relocate to nearby, less expensive areas. Agents move incrementally toward the periphery to mitigate congestion while still benefiting from proximity to the core. In equilibrium, this tension gives rise to a single-peaked monocentric spatial pattern, characterized by a dominant center surrounded by lower-density fringes, as Fig. 2B illustrates.

By contrast, "global" dispersion forces spill *across* locations, and are inherently spatial in nature. A key example is market crowding arising from interregional trade in the presence of immobile factors, such as land or other natural resources. Through trade, a large central city can extend its agglomeration advantages beyond its boundaries

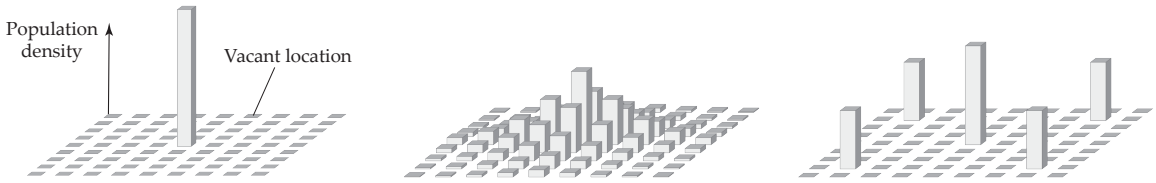

(A) Full agglomeration (B) Monocentric distribution (C) Polycentric distribution

Figure 2: Spatial distributions in a square economy with uniform local fundamentals.

and dominate nearby markets, making those locations unattractive for firms. However, if trade frictions are relatively high, peripheral locations offer protection from such negative effects. Firms relocate to these protected markets to serve local demand, subsequently re-agglomerating to capture local scale economies. These emerging economic agglomerations compete for market access and resources, effectively repelling one another across space. In equilibrium, multiple agglomerations emerge, as shown in Fig. 2C.

As transport costs decline, local and global dispersion forces act in opposite directions. At the global scale, winners and losers emerge. Improved transport connectivity expands the spatial reach of firms and consumers, intensifying interregional market competition. This increased competition tends to disadvantage smaller agglomerations, leading economic activity to become more concentrated in a limited number of large centers. At the local scale, by contrast, lower transport costs reduce the relative advantage of proximity, strengthening congestion forces within cities and encouraging spatial dispersion within each agglomeration. Together, these mechanisms can give rise to a dual spatial pattern: greater concentration across regions combined with decentralization within individual agglomerations.

Distinguishing between local and global dispersion forces helps clarify the equilibrium spatial patterns implied by models of economic agglomeration and the comparative statics they generate. A wide range of spatial models can be classified into three broad types: models with only local dispersion force ("Type L"), models with only global dispersion forces ("Type G"), and models that incorporate both ("Type LG"). These model classes yield fundamentally different predictions about how declining transport costs shape the spatial economy. Reflecting the basic mechanisms discussed above, Type L models predict that lower transport costs primarily induce within-city decentralization. Type G models predict increased regional concentration. Type LG models combine these two effects and predict the dual response discussed earlier.

These theoretical distinctions carry significant implications for the counterfactual analysis conducted in quantitative spatial models (QSMs). QSMs can produce sharply

divergent counterfactual outcomes depending on the dispersion forces they embed. For example, lower transport costs tend to promote spatial spread across locations when local dispersion forces dominate (e.g., Helpman, 1998; Allen and Arkolakis, 2014), but promote further agglomeration toward central locations when global dispersion forces are primary (e.g., Krugman, 1991). Whether transport improvements lead to spatial spreading or further concentration depends on the spatial scale at which dispersion forces operate. Thus, transport policies intended to support peripheral regions may succeed or backfire depending on whether the models guiding these policies adequately capture the relevant dispersion forces.

2 The two-region economy

To introduce key concepts, we consider two-location models throughout this section, and proceed to many-location settings in Sections 3 and 4.

Preliminaries. There are perfectly mobile *agents* (e.g., households) who choose their location to maximize utility. Throughout, locations are called *regions* for convenience. Let $x_i \geq 0$ denote the continuous mass of agents in the region $i \in \{1,2\}$, where $x_1 + x_2 = 1$. The indirect utility of agents in the region i is a differentiable function of the spatial distribution $\boldsymbol{x} = (x_1, x_2)$ and is indicated by $v_i(\boldsymbol{x})$. A *spatial equilibrium* is a spatial distribution $\boldsymbol{x}^*$ in which no agent is motivated to relocate. For example, if $x_1^*, x_2^* > 0$, then $\boldsymbol{x}^*$ is a spatial equilibrium if and only if $v_1(\boldsymbol{x}^*) = v_2(\boldsymbol{x}^*)$. A spatial equilibrium is *stable* if the economy returns to it following any marginal migration shock. As will become clear in our subsequent analysis, a spatial equilibrium is not necessarily stable in the presence of self-reinforcing agglomeration forces.

Transport between regions is costly, and $\phi \in (0,1)$ measures the *ease of transport* between regions. Higher values of ϕ indicate better access. For later use, we also introduce the *proximity matrix* $[\phi_{ij}]$ following Matsuyama (2017), where $\phi_{ij} \in (0,1]$ is the ease of transport from region i to j. For the two-region case in this section,

$$\begin{bmatrix} \phi_{11} & \phi_{12} \\ \phi_{21} & \phi_{22} \end{bmatrix} = \begin{bmatrix} 1 & \phi \\ \phi & 1 \end{bmatrix}. \tag{1}$$

To focus on forces driven by transport costs and the endogenous spatial distribution of agents, region-specific characteristics (e.g., innate amenity or productivity) are assumed to be homogeneous. With these common settings in place, we consider a series of specifications for $\boldsymbol{v}(\boldsymbol{x}) = (v_1(\boldsymbol{x}), v_2(\boldsymbol{x}))$, including general equilibrium models such as Krugman (1991); Helpman (1998); Tabuchi (1998); Redding and Sturm (2008); Allen

and Arkolakis (2014), to illustrate the core ideas.

2.1 The Beckmann model: A "local" dispersion force

We start with the following parsimonious specification:

$$v_i(\boldsymbol{x}) = x_i^{-\beta}\Big(\sum_j \phi_{ij} x_j\Big)^{\alpha} \qquad (\alpha, \beta > 0). \tag{2}$$

The first term, $x_i^{-\beta}$, captures the localized congestion force within each region, while the second term is positive externalities between regions or the agents' desire to be close to each other. We call this the Beckmann model, following Beckmann (1976).[3]

The symmetric distribution of agents, $\bar{\boldsymbol{x}} = (\frac{1}{2}, \frac{1}{2})$, is always a spatial equilibrium. In fact, if we define the utility difference between the two regions by

$$\Delta(\boldsymbol{x}) \equiv v_1(\boldsymbol{x}) - v_2(\boldsymbol{x}), \tag{3}$$

we confirm $\Delta(\bar{\boldsymbol{x}}) = 0$.

While $\bar{\boldsymbol{x}}$ is an equilibrium, with both agglomeration and dispersion forces, $\bar{\boldsymbol{x}}$ is not stable if the former dominates the latter. To assess the stability of $\bar{\boldsymbol{x}}$, we examine the incentive of movers. Consider a small mass of agents moving from region 2 to 1, so that x_1 rises and x_2 falls symmetrically. If Δ decreases under this perturbation, then $\Delta < 0$ after the move: utility in region 2 exceeds that in region 1, and the movers will prefer to return. This induces a restoring force and hence $\bar{\boldsymbol{x}}$ is locally stable. If Δ increases, then $\Delta > 0$ after the move: the movers prefer to stay in region 1, and the deviation attracts additional movers now that the utility is higher in region 1. Hence, $\bar{\boldsymbol{x}}$ is unstable.

Figure 3 illustrates the above discussion. The symmetric equilibrium $\bar{\boldsymbol{x}}$ is stable in the left panel. In the right panel, $\bar{\boldsymbol{x}}$ is unstable and two additional stable spatial equilibria arise, each exhibiting *endogenous agglomeration*, in which one region becomes larger despite the perfect symmetry of the regional fundamentals.

We can formalize the above discussion by a simple stability criterion.[4]

[3] Beckmann (1976) studied spatial agglomeration arising from a trade-off between local crowding effects and spatial interactions among urban dwellers. Closely related ideas were explored in Papageorgiou and Smith (1983). The Beckmann model can be viewed as a precursor to richer models such as Fujita and Ogawa (1982) and Lucas and Rossi-Hansberg (2002), which in turn form the foundation of modern quantitative urban models (Redding, 2025a). While Beckmann's original analysis is conducted in continuous space, we consider a discrete-space, multiplicative analogue to streamline the exposition.

[4] All omitted proofs are in Appendix A.

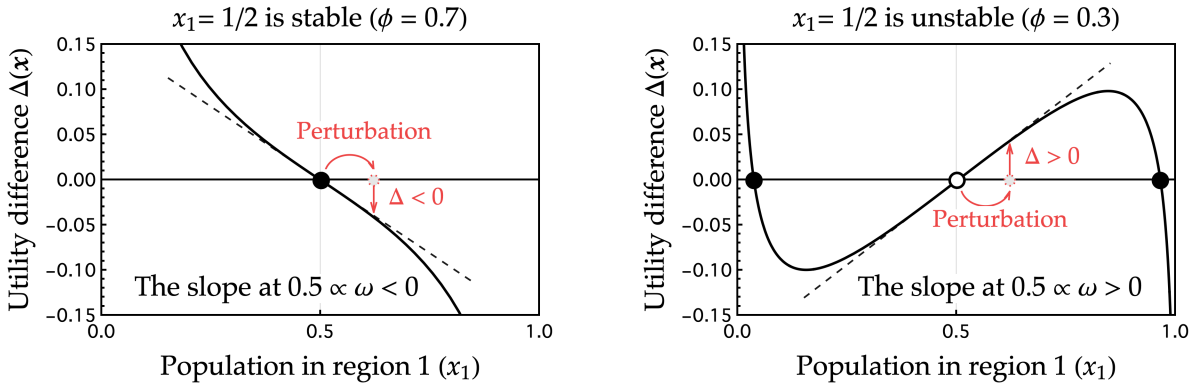

Figure 3: Stability of the symmetry in the Beckmann model ($\alpha = 1/2, \beta = 1/6$)

Lemma 1. Given a differentiable v, define the *utility gain* for marginal movers by

$$\omega \equiv \frac{\bar{x}}{\bar{v}} \cdot \frac{\partial \Delta(\boldsymbol{x})}{\partial x_1}\bigg|_{\boldsymbol{x}=\bar{\boldsymbol{x}}} = \frac{\bar{x}}{\bar{v}} \cdot \left(\frac{\partial v_1(\boldsymbol{x})}{\partial x_1} - \frac{\partial v_2(\boldsymbol{x})}{\partial x_1}\right)\bigg|_{\boldsymbol{x}=\bar{\boldsymbol{x}}}, \tag{4}$$

where $\bar{x} \equiv \frac{1}{2}$ and $\bar{v} = v_1(\bar{\boldsymbol{x}}) = v_2(\bar{\boldsymbol{x}}) > 0$. Then, the symmetric equilibrium $\bar{\boldsymbol{x}}$ is stable if $\omega < 0$, and unstable if $\omega > 0$. ■

In Eq. (4), normalization by $\bar{x}/\bar{v}$ only simplifies the final expression of ω.

In the Beckmann model, we compute

$$\omega = -\beta + \alpha\Theta, \qquad \text{where} \qquad \Theta \equiv \frac{1-\phi}{1+\phi} \in (0,1). \tag{5}$$

The negative term $-\beta$ represents the dispersion force, while the positive term $\alpha\Theta$ represents the agglomeration force. The sign of ω, and hence the stability of $\bar{\boldsymbol{x}}$, depends on which force dominates: $\bar{\boldsymbol{x}}$ is stable if $\beta > \alpha\Theta$, and unstable if $\beta < \alpha\Theta$.

In Eq. (5), the dispersion force does not depend on ϕ because it is not affected by interregional transport conditions. By contrast, the agglomeration force depends on ϕ as it incorporates interregional interactions. In particular, $\alpha\Theta$ decreases as ϕ increases. That is, the benefit of becoming close to others is small if transport is less costly.[5]

Importantly, Θ itself is the *proximity gain* for marginal movers at each ϕ. To see this, set $\alpha = 1$ and $\beta = 0$. Then, $v_i(\boldsymbol{x}) = \sum_j \phi_{ij} x_j$ corresponds to a parsimonious measure of proximity. Since $\omega = \Theta$ in this case, Θ indeed represents the proximity gain.

With Eq. (5), we can determine the stability of $\bar{\boldsymbol{x}}$ in the Beckmann model. If $\beta \geq \alpha$, congestion force is so strong that $\omega < 0$ for all $\phi \in (0,1)$. Agglomeration cannot occur, as $\bar{\boldsymbol{x}}$ is always stable. If $0 < \beta < \alpha$, the level of ϕ matters. As Fig. 3 illustrates, $\bar{\boldsymbol{x}}$ is stable if ϕ is large (i.e., if the agglomeration force is small), and unstable otherwise.

[5] If instead the regions are in autarky ($\phi = 0$), the agglomeration force reduces to local spillovers à la Henderson (1974). Since $\Theta = 1$ and $\alpha\Theta = \alpha$, the stability condition is whether $\alpha < \beta$ or not.

Gain functions. Beyond the Beckmann model, the utility gain ω in Lemma 1 is well defined for any differentiable v. In many spatial models, ω is a simple function of Θ,

$$\omega = \Omega(\Theta), \tag{6}$$

as in the Beckmann model. For each model, we call this Ω the *gain function* of the model. The positive terms of Ω represent the model's agglomeration forces, whereas the negative terms represent the dispersion forces. How each term of Ω responds to changes in Θ then describes how transport conditions alter the strengths of these forces, and therefore their relative importance at each transport cost level.[6]

2.2 The Braid model: A "global" dispersion force

To illustrate what gain functions Ω look like under different specifications of the indirect utility function v, we employ another reduced-form model. Consider replacing the local congestion term in the Beckmann model as follows:

$$v_i(\boldsymbol{x}) = y_i(\boldsymbol{x}) \Big(\sum_j \phi_{ij} x_j \Big)^{\alpha}. \tag{7}$$

Here, $y_i(\boldsymbol{x})$ is the income of an agent in the region i. Each region is endowed with one unit of fixed expenditure, which is allocated to all agents according to accessibility. Suppose that the share received by an agent in region i from region m is given by[7]

$$s_{i|m}(\boldsymbol{x}) \equiv \frac{\phi_{im}}{\sum_l x_l \phi_{lm}} \qquad \left(\sum_i x_i \cdot s_{i|m}(\boldsymbol{x}) = 1 \right). \tag{8}$$

Then, we have $y_i(\boldsymbol{x}) = \sum_m s_{i|m}(\boldsymbol{x})$. We refer to the model (7) as the Braid model after Braid (1988) who studied the properties of spatial equilibria for the case $\alpha = 0$.[8]

In this model, proximity to others has a negative impact on the utility of agents, as $s_{i|m}(\boldsymbol{x})$ in Eq. (8) embeds competition between agents in different regions over spatially

[6] Generalization is possible for the cases where the proximity gain is multi-dimensional such as $\boldsymbol{\Theta} \in [0,1]^M$ where M is the number of different interregional interactions. For clarity, we restrict our attention to the case $M = 1$ throughout this study.

[7] Possible microfoundations for the model are abstracted away for brevity.

[8] Braid (1988) analyzed non-monocentric urban structures by modeling spatial competition among a continuum of firms under logit demand, departing from then-standard discrete-firm frameworks (e.g., de Palma et al., 1985). Building on this approach, Takayama and Akamatsu (2011) studied a version of the model (7) and showed that non-monocentric configurations can arise as stable spatial equilibria. Related ideas appear in Harris and Wilson (1978), which proposed a spatial interaction model with gravity-type demand driven by agglomeration and congestion forces. These strands were later unified in general equilibrium models in regional science, notably by Alex Anas and co-authors (e.g., Anas and Kim, 1996; Anas and Xu, 1999; Anas and Liu, 2007).

dispersed expenditure. Concretely, for any combination of $i, j, m \in \{1, 2\}$,

$$\frac{\partial s_{i|m}}{\partial x_j} = -\frac{\phi_{im}}{\sum_l x_l \phi_{lm}} \cdot \frac{\phi_{jm}}{\sum_l x_l \phi_{lm}} = -s_{i|m} \cdot s_{j|m} < 0, \tag{9}$$

demonstrating that a marginal increase in agents in any region $j \in \{1, 2\}$ has negative impacts on $s_{i|m}$. This is simply because such a shock increases the denominator of $s_{i|m}$. Whether income $y_i = \sum_j s_{i|j}$ as a whole increases or not after a migration shock depends on the relative magnitudes of these impacts. Specifically, analogous to the utility gain ω, we can compute the income gain of a marginal mover from region 2 to 1:[9]

$$\frac{\bar{x}}{\bar{y}} \left(\frac{\partial y_1(\boldsymbol{x})}{\partial x_1} - \frac{\partial y_2(\boldsymbol{x})}{\partial x_1} \right) \Bigg|_{\boldsymbol{x}=\bar{\boldsymbol{x}}} = -\frac{1+\phi^2}{(1+\phi)^2} + \frac{2\phi}{(1+\phi)^2} = -\frac{(1-\phi)^2}{(1+\phi)^2} = -\Theta^2 < 0, \tag{10}$$

where $\bar{y} = y_1(\bar{\boldsymbol{x}}) = y_2(\bar{\boldsymbol{x}}) = 1/\bar{x}$. This shows that a marginal migration shock always induces an income *loss* for the movers. This force is on the second order of Θ, reflecting that the proximity matrix $[\phi_{ij}]$ appears twice in the numerator of Eq. (9).

From Eqs. (4) and (10), the utility gain for the Braid model is given as follows:

$$\omega = \alpha\Theta - \Theta^2. \tag{11}$$

The gain function for the model is therefore $\Omega(\Theta) = \alpha\Theta - \Theta^2$. The first term is the same agglomeration force as in the Beckmann model. The second term, $-\Theta^2$, represents the "global" dispersion force due to the income loss in Eq. (10).

This dispersion force weakens as Θ falls (i.e., as ϕ increases). If ϕ is very small, regions are effectively in autarky and $y_i \approx s_{i|i} \approx 1/x_i$. In this case, a migration shock that raises x_i directly intensifies local competition and lowers income, creating a strong incentive to disperse ($-\Theta^2 \approx -1$). By contrast, if ϕ is close to one, regions face nearly identical crowding conditions ($y_i \approx 1$), and migration shocks have little effect on income ($-\Theta^2 \approx 0$).

In the model, $\bar{\boldsymbol{x}}$ can become unstable for some ϕ whenever $\alpha > 0$. If $0 < \alpha < 1$, $\bar{\boldsymbol{x}}$ is stable for high transport costs (large $\Theta \Leftrightarrow$ small ϕ) and unstable for low transport costs (small $\Theta \Leftrightarrow$ large ϕ). If $\alpha \geq 1$, $\bar{\boldsymbol{x}}$ is unstable for all ϕ.

Contrasting implications of transportation costs. The two reduced-form models yield fundamentally opposing implications. In the Beckmann model, $\bar{\boldsymbol{x}}$ is stable for low transport costs (large ϕ), and agglomeration occurs for high transport costs (small ϕ). The Braid model exhibits the opposite behavior. Figures 4A and 4B confirm this by showing the full equilibrium paths on the ϕ-axis. The contrast persists in the presence

[9] From Eq. (9), $\frac{\partial y_1}{\partial x_1} = -(s_{1|1})^2 - (s_{1|2})^2 = -\frac{1+\phi^2}{\bar{x}^2(1+\phi)^2}$ and $\frac{\partial y_2}{\partial x_1} = -s_{2|1} \cdot s_{1|1} - s_{2|2} \cdot s_{1|2} = -\frac{2\phi}{\bar{x}^2(1+\phi)^2}$.

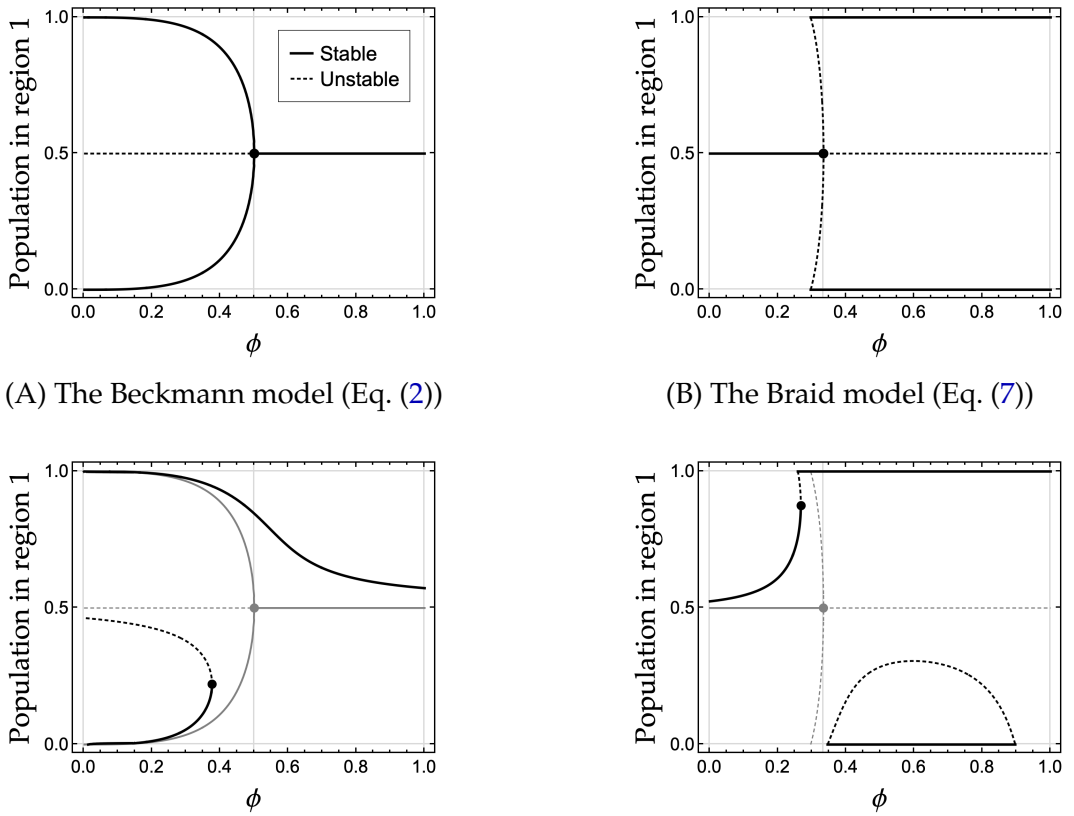

(A) The Beckmann model (Eq. (2))

(B) The Braid model (Eq. (7))

(C) The Beckmann model with asymmetry

(D) The Braid model with asymmetry

Figure 4: Equilibrium values of x_1 in the Beckmann model and the Braid model

Note: We set $\alpha = 1/2$ for both models, and $\beta = 1/6$ for the Beckmann model. In Panels (A) and (B), the black markers indicate the points where the symmetry becomes unstable. In Panels (C) and (D), we multiply $v_1(\boldsymbol{x})$ by 1.05. The black markers indicate the points at which stable and unstable equilibrium curves converge. For reference, the equilibria for the symmetric cases are shown in light gray.

of asymmetries. For instance, if region 1 possesses an exogenous advantage as in Figs. 4C and 4D, a symmetric configuration is no longer an equilibrium. Nevertheless, the qualitative findings remain consistent with the symmetric case: an increase in ϕ (declining transport costs) fosters dispersion in the Beckmann model but drives agglomeration in the Braid model.

This divergence is rooted in the different spatial scales of dispersion forces. In the Beckmann model, dispersion under high ϕ is driven by the relative weakening of the agglomeration force, whereas the "local" dispersion force remains invariant to ϕ. In the Braid model, endogenous agglomeration occurs due to the relative decline of the "global" dispersion force as ϕ increases. Thus, the spatial scale of the dominant dispersion force can alter the implications of declining transport costs.[10] As noted in

[10]In fact, the literature on two-region models has recognized that various dispersion mechanisms can have opposing effects. For example, Fujita and Thisse (2013, Ch.8) compares the seminal models by Krugman (1991) and Helpman (1998) and noted that "Krugman's scenario is reversed" (p.289) in Helpman-type frameworks with urban costs. This point is revisited also in the recent survey by Allen and Arkolakis (2025) (pp.26–27).

the introduction and further discussed in Section 3, in many-region settings, these two types of dispersion forces lead to contrasting spatial patterns.

2.3 Benefit matrix and the spatial scale of economic forces

While the insights from the stylized models considered so far are intuitive and nearly immediate, they rely on a reduced-form structure. In more comprehensive frameworks, particularly general equilibrium models where wages, prices, and land rents are endogenously determined, the impact of transport costs becomes considerably more complex. In such settings, multiple forces interact simultaneously, making it difficult to isolate whether "local" or "global" dispersion dominates.

To bridge the gap between our stylized insights and richer general equilibrium specifications, it is necessary to develop a formal method for evaluating how these endogenous forces respond to changes in transport costs. For this purpose, we introduce an analytical tool termed the *benefit matrix*. This matrix allows us to systematically decompose the spatial externalities inherent in spatial models and classify them into the local and global forces in our earlier discussion.

Definition 1 (Benefit matrix)**.** For a differentiable indirect utility function v, its *benefit matrix* $\mathbf{V}$ is its elasticity matrix at symmetric equilibrium $\mathbf{V} \equiv \frac{\bar{x}}{\bar{v}}[\frac{\partial v_i}{\partial x_j}(\bar{\boldsymbol{x}})]_{i=1,2;j=1,2}$.

Then, the utility gain ω in the symmetric equilibrium $\bar{\boldsymbol{x}}$ is the eigenvalue of the benefit matrix $\mathbf{V}$, associated with the eigenvector $\boldsymbol{z} = (1, -1)$. Intuitively, $\boldsymbol{z}$ represents the direction of possible migration shocks because $(\bar{x} + \epsilon, \bar{x} - \epsilon) = \bar{\boldsymbol{x}} + \epsilon \boldsymbol{z}$.

Example 1. Consider the Beckmann model. Its benefit matrix is

$$\mathbf{V} = -\beta \mathbf{I} + \alpha \mathbf{D}, \tag{12}$$

where $\mathbf{I}$ is the identity matrix and $\mathbf{D}$ is the *row-normalized proximity matrix*:

$$\mathbf{D} = \frac{1}{1+\phi} \begin{bmatrix} 1 & \phi \\ \phi & 1 \end{bmatrix}. \tag{13}$$

We confirm $\mathbf{D}\boldsymbol{z} = \frac{1-\phi}{1+\phi}\boldsymbol{z} = \Theta \boldsymbol{z}$. That is, $\boldsymbol{z} = (1, -1)$ is an eigenvector of $\mathbf{D}$, and the proximity gain Θ is the associated eigenvalue. Then, $\mathbf{V}\boldsymbol{z} = (-\beta + \alpha\Theta)\boldsymbol{z} = \omega \boldsymbol{z}$ from Eq. (12), showing that ω is indeed an eigenvalue of $\mathbf{V}$ corresponding to $\boldsymbol{z}$. ■

Example 2. The benefit matrix for the Braid model is

$$\mathbf{V} = \alpha \mathbf{D} - \mathbf{D}^2., \tag{14}$$

Since $\mathbf{V}\boldsymbol{z} = (\alpha\Theta - \Theta^2)\boldsymbol{z}$, $\omega = \alpha\Theta - \Theta^2$ is the eigenvalue of $\mathbf{V}$ associated with $\boldsymbol{z}$. ■

Examples 1 and 2 illustrate that the gain function Ω introduced earlier (Eq. (6)) arises from the structure of $\mathbf{V}$. The utility gain takes the form $\omega = \Omega(\Theta)$ because the benefit matrix itself can be written in parallel form $\mathbf{V} = \Omega(\mathbf{D})$. Here, the matrix function is interpreted in a straightforward way, e.g., matrix polynomials. We can thus think of $\mathbf{V} = \Omega(\mathbf{D})$ and $\omega = \Omega(\Theta)$ interchangeably.

In the two reduced-form examples, the gain function $\Omega(\Theta)$ allows us to formally distinguish the spatial scale of the economic forces. A negative constant term in the gain function $\Omega(\Theta)$ corresponds to a *local* dispersion force. In contrast, negative non-constant terms correspond to *global* dispersion forces. The spatial scale for agglomeration forces can be similarly defined: positive constants are local agglomeration forces, and negative non-constant terms are global agglomeration forces.

2.4 General equilibrium models

We now examine specific models in the literature to illustrate that their benefit matrices $\mathbf{V}$ are simple functions of $\mathbf{D}$. We can then immediately obtain the associated gain functions and determine the spatial scale of the dispersion forces in each model. Detailed derivations are provided in Online Appendix F.

The Helpman (1998) / Redding and Sturm (2008) model. Helpman considered an imperfectly competitive framework in which agents consume both differentiated tradable goods and local non-tradable goods (i.e., housing). We consider its variant by Redding and Sturm. The indirect utility of mobile workers in this model is

$$v_i(\boldsymbol{x}) = x_i^{-(1-\mu)} w_i^{\mu} \cdot \mathrm{CMA}_i^{\frac{\mu}{\sigma-1}}, \tag{15}$$

where $\mu \in (0,1)$ is consumers' expenditure share on tradables and $1-\mu \in (0,1)$ is that on non-tradables, $\sigma > 1$ is the elasticity of substitution of horizontally differentiated tradable varieties, w_i is the nominal wage in region i, and $\mathrm{CMA}_i \equiv \sum_{j\in\mathcal{I}} x_j w_j^{1-\sigma} \phi_{ji}$ is the so-called "consumer market access." The proximity matrix is $\phi_{ij} = \tau_{ij}^{1-\sigma}$, where $\tau_{ij} \geq 1$ is the iceberg trade cost from region i to j. Given $\boldsymbol{x}$, the wage $\boldsymbol{w} = (w_i)$ is endogenously determined in general equilibrium with interregional trade.

The benefit matrix for this model can be computed as follows:

$$\mathbf{V} = C(\mathbf{D}) \cdot \left(-(1-\mu)\mathbf{I} + c_1 \mathbf{D}\right), \tag{16}$$

where $C(\mathbf{D}) \equiv \left(\mathbf{I} + \frac{\sigma-1}{\sigma}\mathbf{D}\right)^{-1}$ and $c_1 \equiv \frac{\mu}{\sigma-1} + \frac{\mu}{\sigma} - (1-\mu)\frac{\sigma-1}{\sigma}$. This then implies

$$\omega = C(\Theta) \cdot (-(1-\mu) + c_1\Theta) \tag{17}$$

where $C(\Theta) \equiv (1 + \frac{\sigma-1}{\sigma}\Theta)^{-1} > 0$. Since $C(\Theta) > 0$, the sign of ω hinges on the sign of

$$\omega^\sharp \equiv -(1-\mu) + c_1\Theta, \tag{18}$$

which is similar to the Beckmann model. In particular, $-(1-\mu)$ corresponds to the *local dispersion force* due to crowding in the non-tradables market in each region. If μ is sufficiently large, then agents' love for variety produces a strong *global agglomeration force*: we have $c_1 > 0$ and hence $c_1\Theta > 0$ if $\mu > (\frac{\sigma-1}{\sigma})^2$, where we note $\frac{\sigma-1}{\sigma} \in (0,1)$. If further $\mu > \frac{\sigma-1}{\sigma}$, $\bar{\boldsymbol{x}}$ is unstable for high transport costs (large Θ) and stable for low transport costs (small Θ), just as in the Beckmann model.

We provide a slightly detailed derivation behind the final expressions (16) and (17) for illustration. The definition of $\boldsymbol{v}$ in Eq. (15) yields

$$\mathbf{V} = -(1-\mu)\mathbf{I} + \mu\mathbf{W} + \frac{\mu}{\sigma-1}\left(\mathbf{D} - (\sigma-1)\mathbf{D}\mathbf{W}\right). \tag{19}$$

The first term in Eq. (19) represents the crowding in the housing markets. The second is the direct impact of nominal income on indirect utility, where

$$\mathbf{W} = \frac{1}{\sigma}C(\mathbf{D}) \cdot \mathbf{D} \tag{20}$$

is the elasticity matrix of nominal wages.[11] The third term in Eq. (19) is the "cost-of-living" effects: the price index in a region falls when nearby regions offer a greater variety of goods but increases when they pay higher wages and thus charge higher prices (see, e.g., Fujita and Thisse, 2013; Baldwin et al., 2003; Brakman et al., 2019).

Substituting Eq. (20) into Eq. (19) and rearranging, we obtain

$$\mathbf{V} = -(1-\mu)\mathbf{I} + \frac{\mu}{\sigma-1}\mathbf{D} + \frac{\mu}{\sigma}(\mathbf{I}-\mathbf{D}) \cdot C(\mathbf{D}) \cdot \mathbf{D} \quad \text{and hence} \tag{21}$$

$$\omega = \Omega(\Theta) = \underbrace{-(1-\mu)}_{<0} + \underbrace{\frac{\mu}{\sigma-1}\Theta}_{>0} + \underbrace{\frac{\mu}{\sigma}C(\Theta)(1-\Theta)\Theta}_{>0}. \tag{22}$$

The first two terms represent the partial equilibrium utility gains where wage adjust-

[11] Concretely, $\mathbf{W} \equiv \frac{\bar{x}}{\bar{w}}\left[\frac{\partial w_i}{\partial x_j}(\bar{\boldsymbol{x}})\right]_{i=1,2;j=1,2}$ with $\bar{w} = w_1(\bar{\boldsymbol{x}}) = w_2(\bar{\boldsymbol{x}})$. As $C(\mathbf{D}) = \left(\mathbf{I} + \frac{\sigma-1}{\sigma}\mathbf{D}\right)^{-1}$ plays a role analogous to the Leontief inverse in input–output analysis, $\mathbf{W}$ captures the general equilibrium response of wages to marginal migration shocks taking into account interregional trade.

ments are ignored. The third term in Eq. (22) summarizes the *net* impact of wages on indirect utility in general equilibrium, both through the (positive) individual-level income gain and the (negative) cost-of-living effect. It is a net global agglomeration force because it is strictly positive for all $\Theta \in (0,1)$. Thus, the only dispersion force that can stabilize $\bar{x}$ is the local dispersion force captured by the first term of Eq. (22).

Further rearrangement of Eqs. (21) and (22) yields the final expressions (16) and (17). By construction, $\omega^\sharp$ in Eq. (18) captures the *net* utility gain considering all endogenous forces and their general equilibrium trade-offs. For example, despite there is no *net* global dispersion force, $\omega^\sharp = -(1-\mu) + c_1\Theta$ has a negative term involving Θ:

$$c_1\Theta = \frac{\mu}{\sigma}\Theta + \frac{\mu}{\sigma-1}\Theta \underbrace{-(1-\mu)\frac{\sigma-1}{\sigma}\Theta}_{<0} \tag{23}$$

This last term represents how the local dispersion force $-(1-\mu)$ counteract, in each agent's migration incentives, the core agglomeration forces in the model, such as the love for variety and demand linkage (the first two terms of Eq. (23)).

The Allen and Arkolakis (2014) model. The model is a perfectly competitive framework with both positive and negative externalities. Appendix F.2.4 shows that the benefit matrix for the Allen–Arkolakis model is

$$\mathbf{V} = C(\mathbf{D}) \cdot (c_0\mathbf{I} + c_1\mathbf{D}), \tag{24}$$

where $C(\mathbf{D}) \equiv ((\sigma\mathbf{I} + (\sigma-1)\mathbf{D})(\mathbf{I}-\mathbf{D}))^{-1}$, $c_0 \equiv \alpha - \beta - \frac{1+\alpha}{\sigma}$, and $c_1 \equiv \alpha - \beta + \frac{1+\beta}{\sigma}$. The parameters $\alpha > 0$ and $\beta > 0$ are the magnitudes of local agglomeration and congestion effects with respect to local population, respectively, and $\sigma > 1$ is the elasticity of substitution across regionally differentiated goods. The gain function Ω is obtained accordingly. Analogous to the Helpman model, the sign of ω depends on a linear expression $\omega^\sharp \equiv c_0 + c_1\Theta$ that captures the net migration incentive for agents.

If the dispersion force is relatively strong (relatively large β), we have $c_0 < 0$, indicating a *net* local dispersion force. Likewise, if the agglomeration force is relatively strong (relatively large α), we have $c_1 > 0$, indicating a *net* global agglomeration force. In particular, if $\beta < \alpha < \bar{\alpha} \equiv \frac{\beta\sigma+1}{\sigma-1}$, agglomeration occurs if transport costs are high (small ϕ) and dispersion occurs if transport costs are low (large ϕ). Under the presence of externalities, the only stabilizing force in the Allen–Arkolakis model is the local crowding effect.[12] That is, as discussed in Allen and Arkolakis (2014), this model bears

[12] In the special case where $\alpha = 0$ and $\beta = 0$, the model reduces to the Armington (1969) framework. For this case, $\omega = \frac{1}{\sigma}C(\Theta)(-1+\Theta) < 0$, and the net agglomeration term $(-1+\Theta)$ does not contain any negative components in Θ. Nonetheless, ω is a negative function and can be interpreted as the

a structural similarity to the Helpman model.

The Krugman (1991) model. Krugman's seminal model emphasizes the role of market crowding. In this model, there is always a nonzero demand for the manufacturing goods in each region due to the presence of immobile consumers. This discourages concentration of production in one region if transport costs are high, and this produces a global dispersion force as in the Braid model. For this model, the benefit matrix is

$$\mathbf{V} = \mathbf{W} + \frac{\mu}{\sigma - 1}\left(\mathbf{D} - (\sigma - 1)\mathbf{D}\mathbf{W}\right) \tag{25}$$

where the elasticity matrix for the nominal wage is

$$\mathbf{W} = \frac{1}{\sigma}C(\mathbf{D}) \cdot \left(\mu\mathbf{D} - \mathbf{D}^2\right), \quad \text{where} \quad C(\mathbf{D}) \equiv \left(\mathbf{I} - \frac{\mu}{\sigma}\mathbf{D} - \frac{\sigma - 1}{\sigma}\mathbf{D}^2\right)^{-1}. \tag{26}$$

Compared to Eq. (19), the local dispersion force is absent. Compared with Eqs. (20) and (26), the Krugman model has a negative term $-\mathbf{D}^2$, while the Helpman model does not. We can rearrange $\mathbf{V}$ to see

$$\mathbf{V} = C(\mathbf{D}) \cdot \left(c_1\mathbf{D} - c_2\mathbf{D}^2\right). \tag{27}$$

where $c_1 \equiv \frac{\mu}{\sigma-1} + \frac{\mu}{\sigma} > 0$ and $c_2 \equiv \frac{\mu^2}{\sigma-1} + \frac{1}{\sigma} > 0$. The gain function is then $\omega = C(\Theta) \cdot (c_1\Theta - c_2\Theta^2)$ with $C(\Theta) \equiv (1 - \frac{\mu}{\sigma}\Theta - \frac{\sigma-1}{\sigma}\Theta^2)^{-1} > 0$, where the core trade-off is captured by $\omega^\sharp \equiv c_1\Theta - c_2\Theta^2$. The first term $c_1\Theta > 0$ represents global agglomeration forces, and the second term $-c_2\Theta^2 < 0$ captures global dispersion forces augmented by immobile demands. As in the Braid model, dispersion is preferred if transport costs are high (small ϕ), and agglomeration occurs otherwise (large ϕ).

The Tabuchi (1998) model. Tabuchi integrated urban costs into Krugman's framework with immobile consumers. In addition to the regional-scale component of Krugman, each region has an Alonso–Muth–Mills monocentric city structure. Within each region, agents commute to a central business district and face the trade-off between commuting costs and land rent. The benefit matrix for the Tabuchi model reduces to

$$\mathbf{V} = C(\mathbf{D}) \cdot \left(-c_0\mathbf{I} + c_1\mathbf{D} - c_2\mathbf{D}^2\right), \tag{28}$$

where $C(\mathbf{D})$ is a matrix factor that captures general equilibrium effects, and $c_0 = \gamma\epsilon_1 > 0$, $c_1 = \frac{\mu}{\sigma-1} + \frac{\mu}{\sigma} > 0$, and $c_2 = \frac{\mu^2}{\sigma-1}\epsilon_2 + \frac{1}{\sigma}\epsilon_3$. Here, γ is the share of housing expenditures, and $\epsilon_1, \epsilon_2, \epsilon_3$ capture the effects of urban costs. For example, the larger

underlying "global dispersion force" inherent to general equilibrium in the Armington framework.

the commuting cost parameter and/or the opportunity cost of the land, the larger $\epsilon_1 > 0$ becomes, so that the local dispersion force $-c_0$ becomes more pronounced. The stability of $\bar{\boldsymbol{x}}$ depends on the quadratic expression $\omega^\sharp \equiv -c_0 + c_1\Theta - c_2\Theta^2$.

The agglomeration force ($c_1\Theta > 0$) is the same as the Krugman model, while $-c_0 < 0$ captures the local dispersion force due to urban costs. The term $c_2\Theta^2$ captures net global forces that include the impacts of urban costs through general equilibrium. The model features both local and global dispersion forces, and the symmetric equilibrium can be stable for both high and low levels of transport costs.

Idiosyncratic taste shocks. Idiosyncratic preference shocks (McFadden, 1974, 1978a,b) are important both in the quantitative and theoretical literature (Hunt and Simmonds, 1993; Waddell, 2002; Anas and Liu, 2007; Redding and Rossi-Hansberg, 2017; Anas, 1983; Anderson et al., 1992; Tabuchi and Thisse, 2002; Murata, 2003). Regarding taste shocks, Behrens and Murata (2021) demonstrated that the spatial equilibrium condition in models with idiosyncratic shocks can be equivalently represented by that in homogeneous preference models with local non-tradables markets as in Helpman (1998). Thus, from the perspective of stabilizing forces at $\bar{\boldsymbol{x}}$, introducing idiosyncratic shocks into a model with homogeneous preference is equivalent to adding a negative constant to the utility gain ω, i.e., to embedding an additional local dispersion force.[13]

2.5 The three model classes

As the above examples illustrate, for a wide class of spatial models,

$$\mathbf{V} = C(\mathbf{D}) \cdot \left(c_0\mathbf{I} + c_1\mathbf{D} + c_2\mathbf{D}^2\right), \quad \text{and hence} \tag{29}$$

$$\omega = C(\Theta) \cdot \left(c_0 + c_1\Theta + c_2\Theta^2\right), \tag{30}$$

where C and the coefficients $\{c_0, c_1, c_2\}$ are model dependent. In this representation, the stability of $\bar{\boldsymbol{x}}$ is governed by the quadratic term, since the sign of ω is entirely determined by the sign of $c_0 + c_1\Theta + c_2\Theta^2$.

For models of this form, we can define three prototypical classes according to the transport cost conditions under which the symmetric equilibrium is stable: low transport costs (small Θ or large ϕ), high transport costs (large Θ or small ϕ), or both. For convenience, we refer to the three model classes as *Type L*, *Type G*, and *Type LG*, where L and G stand for "local" and "global," respectively.[14]

[13] While equilibrium spatial allocations are the same, the welfare implications of counterfactual shocks may differ between models with homogeneous preferences and those with heterogeneous preferences. See Behrens and Murata (2021) for detailed discussion.

[14] See Appendix A.3 for formal definitions. Here, we restrict our attention to cases in which the

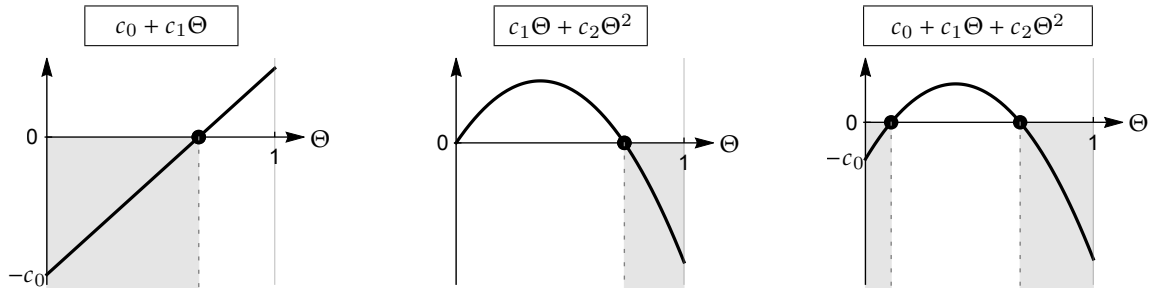

(A) Allen–Arkolakis (Type L) (B) Krugman (Type G) (C) Tabuchi (Type LG)

Figure 5: Representative forms of the quadratic component of the utility gain

Note: For selected examples from the three model types, the "net" utility gain is plotted as a function of the proximity gain Θ. Larger Θ corresponds to smaller ϕ. In each panel, $\bar{x}$ is stable for Θ such that the curve lies below the horizontal axis. The parameter values are chosen such that the stability of $\bar{x}$ depends on Θ. Local dispersion forces stabilize $\bar{x}$ for small Θ, and global dispersion forces for large Θ.

With $\{c_k\}$ being model-dependent constants, we can summarize as follows:

- **Type L** emphasizes local dispersion forces as the dominant dispersion mechanism. The symmetric equilibrium is stable if transport costs are low, and unstable if transport costs are high. $\mathbf{V} = C(\mathbf{D}) \cdot (c_0\mathbf{I} + c_1\mathbf{D})$ with $c_0 < 0$ indicating the local dispersion force.
- **Type G** emphasizes global dispersion forces as the dominant dispersion mechanism. The symmetric equilibrium is stable if transport costs are high, and unstable if transport costs are low. $\mathbf{V} = C(\mathbf{D}) \cdot (c_1\mathbf{D} + c_2\mathbf{D}^2)$, with $c_2 < 0$ representing the global dispersion force.
- **Type LG** has both local and global dispersion forces as the dominant dispersion mechanisms. $\mathbf{V} = C(\mathbf{D}) \cdot (c_0\mathbf{I} + c_1\mathbf{D} + c_2\mathbf{D}^2)$, where $c_0, c_2 < 0$ and $c_1 > 0$. The symmetric equilibrium is stable for both high and low transport cost levels.

Figure 5 illustrates the typical shapes of the quadratic term $c_0 + c_1\Theta + c_2\Theta^2$ in each class, and Table 1 lists representative examples.

The model-dependent coefficients c_0, c_1, c_2 are functions of the model's structural parameters, with transport costs entering only through $\mathbf{D}$. The constant c_0 captures the forces operating *within* regions and therefore represents the local component. The coefficients c_1 and c_2 represent the forces that operate *across* regions. The first-order term c_1 reflects direct interregional effects, such as agglomeration spillovers in the Beckmann model. The quadratic term c_2 captures higher-order spillovers.[15]

agglomeration forces are neither too weak nor too strong, so that the symmetric equilibrium is stable for some values of ϕ and unstable for others.

[15]In many-region settings, c_2 reflects indirect interactions mediated by third regions. For example, in models with interregional trade, agents in the region i are affected by the population of the region j

Model Class	Dominant dispersion force	Stability across transport cost regimes	Examples
Type L	Local	The uniform distribution is stable at low transport costs.	Beckmann (1976) Helpman (1998) Murata and Thisse (2005) Redding and Sturm (2008) Allen and Arkolakis (2014) Redding and Rossi-Hansberg (2017), Section 3
Type G	Global	The uniform distribution is stable at high transport costs.	Harris and Wilson (1978) Krugman (1991) Krugman and Venables (1995) Puga (1999), Section 3 Forslid and Ottaviano (2003) Pflüger (2004)
Type LG	Both local and global	The uniform distribution is stable at both high and low transport costs.	Tabuchi (1998) Fujita et al. (1999a), Section 14.4 Puga (1999), Section 4 Pflüger and Südekum (2008) Pflüger and Tabuchi (2010) Kucheryavyy et al. (2024)

Table 1: Notable examples

Note: The section numbers in the table correspond to those in the referenced papers. For Krugman and Venables (1995) and Puga (1999), the spatial distribution of interest is the share of manufacturing sector. In all the models in the table, the stability of the symmetric equilibrium $\bar{x}$ hinges on the sign of a quadratic function of the form $c_0 + c_1\Theta + c_2\Theta^2$ with model-dependent coefficients $\{c_0, c_1, c_2\}$.

Each coefficient c_k in the c_0, c_1, c_2 representation captures the *composite* general equilibrium effect associated with the corresponding order of $\mathbf{D}$. Its sign therefore reflects the *net* contribution to ω in the order of Θ. For example, if there are both local agglomeration economies and diseconomies, the sign of c_0 reveals which force dominates: $c_0 > 0$ indicates net agglomeration, while $c_0 < 0$ indicates net dispersion. In the Allen–Arkolakis framework, for example, one obtains $c_0 = \alpha - \beta - \frac{1+\alpha}{\sigma}$, and $\alpha < \beta$ is a sufficient condition for the *net* local effect c_0 to be negative.

3 Many regions

This section examines how the proposed taxonomy of spatial models maps to the *endogenous spatial patterns* and their comparative statics in an N-region economy. All variables and functions (e.g., $\boldsymbol{x}$, $\boldsymbol{v}$, $[\phi_{ij}]$, $\mathbf{D}$) are straightforwardly extended. The set of regions is now denoted by $\mathcal{I} \equiv \{1, 2, \ldots, N\}$.

We focus on a stylized geography in which homogeneous regions are symmetrically

because agents in the region i compete with those in the region j for income generated in other regions $k = 1, 2, \ldots$. Such effects typically arise second order in transport frictions, as they depend on the transport costs between regions i and k, as well as between regions j and k.

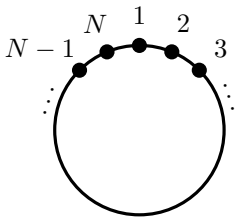

Figure 6: N-region symmetric circle.

placed over a circle and transport is possible only along the circumference (Fig. 6).

Assumption C. The proximity matrix is given by $\phi_{ij} = \phi^{\ell_{ij}}$, where $\phi \in (0,1)$ is the ease of transport between two consecutive regions, and $\ell_{ij} \equiv \min\{|i-j|, N-|i-j|\}$ is the distance between regions i and j over the circumference. All regions are symmetric regarding their local fundamentals (e.g., innate amenity or productivity). In addition, N is a multiple of four.[16] ■

This abstracts away the advantages from each region's unique geographic position, since every region has the same level of geographic accessibility in a circle. Combined with the perfect symmetry in other regional fundamentals, the symmetric distribution $\bar{\boldsymbol{x}} \equiv (\frac{1}{N}, \frac{1}{N}, \ldots, \frac{1}{N})$ is always a spatial equilibrium (Lemma 3 in Appendix A.3).

3.1 The stability of the symmetric equilibrium

Endogenous agglomeration occurs when the symmetric equilibrium $\bar{\boldsymbol{x}}$ is unstable, that is, when it does not withstand small migration shocks. In an economy with N regions, such shocks can be represented as

$$\bar{\boldsymbol{x}} + \epsilon \boldsymbol{z} = (\bar{x} + \epsilon z_1, \bar{x} + \epsilon z_2, \ldots, \bar{x} + \epsilon z_N) \tag{31}$$

where ϵ is a sufficiently small scalar. The vector $\boldsymbol{z} = (z_i)_{i \in \mathcal{I}}$ is a *deviation pattern*: $z_i > 0$ indicates an inflow into region i and $z_i < 0$ an outflow. Since the total population is fixed, we require $\sum_{i \in \mathcal{I}} z_i = 0$. The N-region setting admits a substantially richer set of deviation patterns than the two-region case, because $(\bar{x} + \epsilon, \bar{x} - \epsilon)$ is the only possible perturbation in the two-region setting. Below, we normalize $\|\boldsymbol{z}\| = 1$.

Analogous to the two-region case, the expected utility gains for marginal movers under migration shocks is closely related to the benefit matrix $\mathbf{V} \equiv \left[\frac{\partial v_i}{\partial x_j}(\bar{\boldsymbol{x}})\right]_{i \in \mathcal{I}, j \in \mathcal{I}}$.

Lemma 2. For any deviation pattern $\boldsymbol{z}$ with $\sum_{i \in \mathcal{I}} z_i = 0$ and $\|\boldsymbol{z}\| = 1$, the expected utility gain of marginal movers is $\omega(\boldsymbol{z}) \equiv \boldsymbol{z}^\top \mathbf{V} \boldsymbol{z}$, where $\top$ denotes transpose. ■

[16] This restriction on N is only for expositional simplicity. See Remark 3 in Appendix A.

Then, the value $\omega(\boldsymbol{z})$ characterizes the stability of $\bar{\boldsymbol{x}}$. If $\omega(\boldsymbol{z}) < 0$ for *all* possible deviation patterns, then any migration shock reduces the utility of the movers and $\bar{\boldsymbol{x}}$ is locally stable. If $\omega(\boldsymbol{z}) > 0$ for *some* $\boldsymbol{z}$, the movers benefit from relocating according to that pattern, implying instability. Thus, stability is determined by whether the maximal attainable gain $\omega^* \equiv \max_{\boldsymbol{z}} \omega(\boldsymbol{z})$ is positive or negative.

To characterize ω^*, let $\{\omega_k\}$ denote the eigenvalues of $\mathbf{V}$, and $\{\boldsymbol{z}_k\}$ be their associated eigenvectors. Because $\omega(\boldsymbol{z}_k) = \boldsymbol{z}_k^\top \mathbf{V} \boldsymbol{z}_k = \omega_k \boldsymbol{z}_k^\top \boldsymbol{z}_k = \omega_k \|\boldsymbol{z}_k\|^2 = \omega_k$, we observe

$$\omega^* = \max_k \{\omega_k\}, \tag{32}$$

implying that the largest eigenvalue of $\mathbf{V}$ determines the stability of $\bar{\boldsymbol{x}}$.[17]

How can we obtain $\{\omega_k\}$? Under Assumption C, for all models in Table 1, the benefit matrix satisfies $\mathbf{V} = \Omega(\mathbf{D})$, where the row-normalized proximity matrix $\mathbf{D}$ is replaced by its $N \times N$ counterpart. For each model, the base gain function $\Omega(\Theta)$ is the same as in the case of two-regions.[18] Then, $\mathbf{V}$ and $\mathbf{D}$ share the same set of eigenvectors $\{\boldsymbol{z}_k\}$, and $\mathbf{V} = \Omega(\mathbf{D})$ implies

$$\omega_k = \Omega(\Theta_k), \tag{33}$$

where Θ_k is the eigenvalue of $\mathbf{D}$ corresponding to $\boldsymbol{z}_k$. Each Θ_k is a function of ϕ because ϕ is the only parameter of $\mathbf{D}$ according to our assumptions.

These observations yield a transparent approach to stability analysis, as the following example illustrates.

Example 3. In the Beckmann model, we again have $\mathbf{V} = -\beta \mathbf{I} + \alpha \mathbf{D}$, where $\mathbf{I}$ and $\mathbf{D}$ are replaced by the N-region identity and row-normalized proximity matrices.[19] The kth eigenvalue of $\mathbf{V}$ is then $\omega_k = -\beta + \alpha\Theta_k$ because $\mathbf{D}\boldsymbol{z}_k = \Theta_k \boldsymbol{z}_k$ implies $\mathbf{V}\boldsymbol{z}_k = (-\beta + \alpha\Theta_k)\boldsymbol{z}_k$. The stability of $\bar{\boldsymbol{x}}$ is determined by the sign of $\omega^* = \max_k\{\omega_k\}$. Consider a value of ϕ such that $\bar{\boldsymbol{x}}$ is stable, i.e., $\omega_k < 0$ for all k and hence $\omega^* = \max_k\{\omega_k\} < 0$. Suppose then that ϕ increases or decreases monotonically. Suppose *some* ω_{k*} changes its sign from negative to positive at some ϕ^*. Then, after that point, deviation towards the $\boldsymbol{z}_{k^*}$-direction improves the utility of the movers, and $\bar{\boldsymbol{x}}$ becomes unstable. In this

[17] The discussion here is closely related to Allen et al. (2024). In their framework, the spectral radius of a matrix that collects key model elasticities governs the uniqueness of the equilibrium. In our setting, their uniqueness condition [Theorem 1(a)] corresponds to a sufficient condition for the stability of $\bar{\boldsymbol{x}}$ for all ϕ. This rules out endogenous agglomeration. Our focus instead lies on environments with multiple equilibria [cf. their Theorem 1(c)], and we take a step toward understanding how the underlying network structure shapes the positive properties of these equilibria.

[18] For all models we saw in Section 2.4, the gain functions are derived for the general number of locations under Assumption C, and then specialized to the $N = 2$ case.

[19] Observe that Eq. (2) is defined for general N.

sense, the corresponding eigenvector z_{k^*} represents the critical deviation pattern. ■

3.2 Proximity gains and deviation patterns

The eigenvalues $\{\Theta_k\}$ of $\mathbf{D}$ have a clear interpretation analogous to the proximity gain Θ in the two-region case. Again, for the special case of the Beckmann model with $\beta = 0$ and $\alpha = 1$, the indirect utility function boils down to a simple proximity measure. We have $\mathbf{V} = \mathbf{D}$ and $\omega_k = \Theta_k$, which can be interpreted as follows.

Observation 1. Each eigenvalue Θ_k of $\mathbf{D}$ measures the proximity gain experienced by marginal movers when migration shocks occur in the corresponding direction, z_k. ■

For example, if $N = 4$, the normalized proximity matrix under Assumption C is

$$\mathbf{D} = \frac{1}{1+2\phi+\phi^2}\begin{bmatrix} 1 & \phi & \phi^2 & \phi \\ \phi & 1 & \phi & \phi^2 \\ \phi^2 & \phi & 1 & \phi \\ \phi & \phi^2 & \phi & 1 \end{bmatrix}. \tag{34}$$

There are two relevant eigenvalues:

$$\Theta_1 = \frac{1-\phi}{1+\phi} \quad \text{and} \quad \Theta_2 = \left(\frac{1-\phi}{1+\phi}\right)^2. \tag{35}$$

We can check that there are two eigenvectors associated with Θ_1, namely $z_1^+ = (1, 0, -1, 0)$ and $z_1^- = (0, 1, 0, -1)$. Both represent *monocentric* spatial patterns. For example, in $\bar{x} + \epsilon z_1^- = (\bar{x}, \bar{x}+\epsilon, \bar{x}, \bar{x}-\epsilon)$, one region grows at the expense of another that is two steps away, creating a single center of attraction. For Θ_2, the associated eigenvector is $z_2 = (1, -1, 1, -1)$, and represents a *polycentric* agglomeration pattern $\bar{x} + \epsilon z_2 = (\bar{x}+\epsilon, \bar{x}-\epsilon, \bar{x}+\epsilon, \bar{x}-\epsilon)$. Two regions located two steps apart grow symmetrically, while the two intermediate regions shrink.

There are three intuitive properties about Θ_1 and Θ_2. First, both are positive. Any deviation from the full dispersion induces some form of agglomeration, and for movers this increases the proximity to others. Second, each Θ_k decreases as ϕ increases. The proximity gain decreases if transport costs are less important. Third, $\Theta_1 > \Theta_2$ at any value of ϕ. Naturally, from the perspective of movers, deviation toward a monocentric pattern induces a greater proximity gain than toward a polycentric pattern.

These properties generalize to the N-region case.[20] All $\{\Theta_k\}$ are positive and decrease in ϕ. Each z_k corresponds to a deviation pattern with k symmetric peaks as

[20] Akamatsu et al. (2012), Lemma 4.2, provides the analytical formulae for $\{\Theta_k\}$ and $\{z_k\}$, while the interpretation of $\{\Theta_k\}$ as proximity gains is newly given in the present study. Lemma 5 in Appendix A reproduces the relevant part of the aforementioned lemma, adapted to our context.

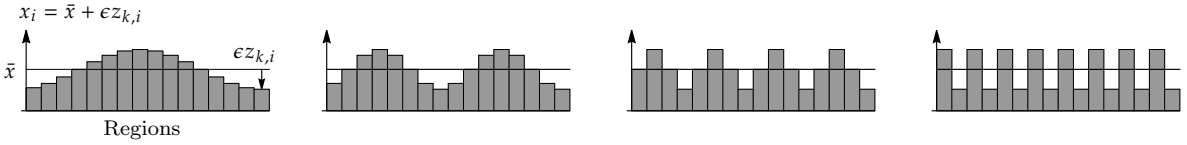

(A) $k = 1$ (B) $k = 2$ (C) $k = 4$ (D) $k = 8$

Figure 7: Examples of spatial patterns generated by $\boldsymbol{z}_k$ ($N = 16$).

illustrated in Fig. 7. Most importantly, the maximum and minimum proximity gains are unambiguously determined: for each ϕ,

$$\max_k \Theta_k = \Theta_1 \quad \text{and} \quad \min_k \Theta_k = \Theta_{\frac{N}{2}}. \tag{36}$$

Intuitively, at any value of ϕ, the monocentric agglomeration pattern ($k = 1$, Fig. 7A) yields the largest proximity gain for the movers. The proximity gain is the smallest if the movers agglomerates in every other region ($k = \frac{N}{2}$, Fig. 7D).

3.3 Contrasting implications for spatial patterns

The relationship (36) has important implications for endogenous spatial patterns. This is because the *maximum* eigenvalue of $\mathbf{D}$ is critical if the model incorporates only local dispersion forces. For instance, since $\omega_k = -\beta + \Theta_k$ in the Beckmann model, we see

$$\omega^* < 0 \quad \Leftrightarrow \quad \max_k \{-\beta + \alpha\Theta_k\} = -\beta + \alpha \max_k \{\Theta_k\} < 0 \quad \Leftrightarrow \quad \Theta_1 < \frac{\alpha}{\beta}. \tag{37}$$

Figure 8A illustrates this for the $N = 8$ case, where we draw curves of ω_k as a function of ϕ. The symmetric equilibrium is stable if Θ_1 is sufficiently small, i.e., if ϕ is sufficiently large. If ϕ monotonically decreases from a high level and crosses ϕ^*, then $\bar{\boldsymbol{x}}$ becomes unstable at ϕ^* because a deviation of the form $\bar{\boldsymbol{x}} + \epsilon \boldsymbol{z}_1$ induces a positive utility gain for the movers. Monocentric agglomeration should form at such a point.

By contrast, if the model has only global dispersion forces, the *minimum* eigenvalue of $\mathbf{D}$ is critical. In the Braid model, $\omega_k = \alpha\Theta_k - \Theta_k^2 = \Theta_k(\alpha - \Theta_k)$, which implies that

$$\omega^* < 0 \quad \Leftrightarrow \quad \max_k \{\alpha - \Theta_k\} = \alpha - \min_k \{\Theta_k\} < 0 \quad \Leftrightarrow \quad \alpha < \Theta_{\frac{N}{2}}. \tag{38}$$

Figure 8B illustrates this for the $N = 8$ case. The symmetric equilibrium is stable if $\Theta_{\frac{N}{2}}$ is sufficiently large, that is, if ϕ is sufficiently small. If ϕ gradually increases from a very small value, at ϕ^*, the $\frac{N}{2}$-centric deviation pattern $\boldsymbol{z}_{\frac{N}{2}}$ becomes attractive for movers.

The two minimal examples show that the *spatial pattern* emerging at the onset of instability is critically dependent on the spatial scale of the dispersion force in the

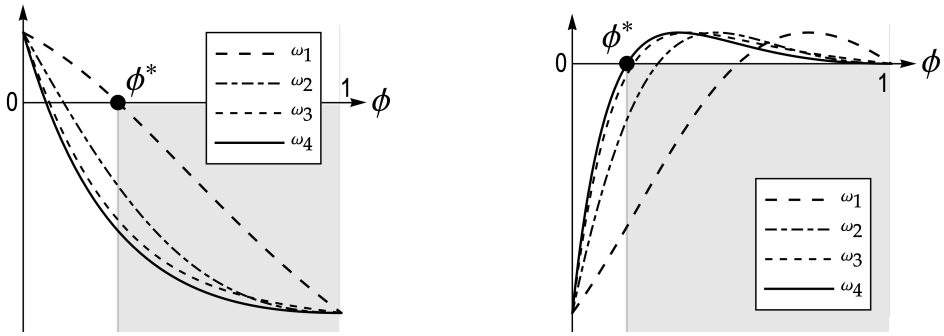

(A) The Beckmann model (Type L) (B) The Braid model (Type G)

Figure 8: Curves of $\omega_k = \Omega(\Theta_k)$ for the two minimal models ($N = 8$, $k = 1, 2, 3, 4$).

Note: The symmetric equilibrium is stable if all curves $\{\omega_k\}_{k=1}^4$ stay below the horizontal axis (gray region). It becomes unstable at ϕ^* where the largest eigenvalue cuts the axis. In the Beckmann model, ω_1 is the first to cross the axis, whereas in the Braid model, it is ω_4.

model. In particular, polycentric patterns arise only when the dispersion force operates at a global scale. This insight from the reduced-form models can be extended to cover general equilibrium models discussed in Section 2.4:

Proposition 1. Suppose Assumption C.

(a) Consider a model of Type L or LG with local dispersion forces. Then, the symmetric equilibrium $\bar{\boldsymbol{x}}$ is stable for large ϕ. Suppose that the model parameters are set so that $\bar{\boldsymbol{x}}$ is stable for all $\phi > \phi^*$ with some threshold value $\phi^* \in (0, 1)$, and becomes unstable at ϕ^*, i.e., $\bar{\boldsymbol{x}}$ is unstable for ϕ slightly smaller than ϕ^*. Then, a single-peaked monocentric spatial equilibrium path branches from $\bar{\boldsymbol{x}}$ at ϕ^*.

(b) Consider a model of Type G or LG with global dispersion forces. Then, $\bar{\boldsymbol{x}}$ can be stable for small ϕ. Suppose that the model parameters are set so that $\bar{\boldsymbol{x}}$ is stable for all $\phi < \phi^*$ with some threshold value $\phi^* \in (0, 1)$, and becomes unstable at ϕ^*, i.e., $\bar{\boldsymbol{x}}$ is unstable for ϕ slightly larger than ϕ^*. Then, a polycentric spatial equilibrium path with $\frac{N}{2}$ symmetric peaks branches from $\bar{\boldsymbol{x}}$ at ϕ^*.

Proposition 1 considers settings in which multiple equilibria may arise, while $\bar{\boldsymbol{x}}$ remains stable for some values of ϕ. This condition need not always hold. For example, in a Type L model with sufficiently strong local dispersion forces, $\bar{\boldsymbol{x}}$ is stable for all $\phi \in (0, 1)$, and the threshold ϕ^* in Proposition 1 (b) does not exist. In such cases, the equilibrium is typically unique, a convenient feature that makes unambiguous counterfactual analysis feasible in quantitative spatial models. Equilibrium uniqueness implies that, absent exogenous geographical asymmetries, $\bar{\boldsymbol{x}}$ is the only possible outcome. At the opposite extreme, in Type G models with sufficiently strong agglomeration forces, $\bar{\boldsymbol{x}}$ can be unstable for all ϕ, leading all agents to concentrate in a single location. Proposition 1 deliberately excludes both of these extremal cases.

3.4 Evolution of spatial patterns

Because Proposition 1 relies on a local stability analysis around $\bar{\boldsymbol{x}}$, it does not establish whether an instability toward polycentric deviations actually leads to stable polycentric equilibria. To trace how stable spatial equilibria evolve as transport costs change beyond Proposition 1, one must specify an indirect utility function, and the resulting characterizations are therefore model dependent.[21]

Nonetheless, in specific models, we can show that polycentric spatial patterns become stable only when global dispersion forces are sufficiently strong, consistent with Proposition 1. This is illustrated by the following formal results and Fig. 9.

Proposition 2. Consider the Type L model of Helpman (1998) on a symmetric four-region circle. Suppose that the full dispersion $\bar{\boldsymbol{x}} = (\frac{1}{4}, \frac{1}{4}, \frac{1}{4}, \frac{1}{4})$ is stable for large ϕ, but that multiple equilibria may exist. Then there exists a threshold $\phi^* \in (0,1)$ such that $\bar{\boldsymbol{x}}$ is unstable for all $\phi \in (0, \phi^*)$. For this range, any duocentric equilibrium of the form (m_1, m_2, m_1, m_2) with $m_1 > m_2$, if it exists, is also unstable, implying that all stable equilibria must be single-peaked. For $\phi \in (\phi^*, 1)$, the fully dispersed allocation $\bar{\boldsymbol{x}}$ is stable, and a single-peaked equilibrium path connects to $\bar{\boldsymbol{x}}$ at ϕ^* [cf. Proposition 1 (a)].

Proposition 3. Consider the Type G model by Forslid and Ottaviano (2003) on a four-region symmetric circle. Assume that the full dispersion $\bar{\boldsymbol{x}} = (\frac{1}{4}, \frac{1}{4}, \frac{1}{4}, \frac{1}{4})$ is stable for small ϕ. Suppose that the initial state is $\bar{\boldsymbol{x}}$, and ϕ increases monotonically from 0. At some threshold ϕ^*, $\bar{\boldsymbol{x}}$ becomes unstable, and duocentric spatial equilibrium of the form (m_1, m_2, m_1, m_2) with $m_1 > m_2$ branches from $\bar{\boldsymbol{x}}$ [cf. Proposition 1 (b)]. In particular, the new stable equilibrium is the duocentric agglomeration such as $(\frac{1}{2}, 0, \frac{1}{2}, 0)$. At some $\phi^{**} > \phi^*$, the duocentric equilibrium becomes unstable. Finally, the full agglomeration in a single region such as $(1, 0, 0, 0)$ becomes the stable spatial equilibrium for large ϕ.

Proof of Propositions 2 and 3. See Akamatsu et al. (2016). □

In Fig. 9, the schematic diagrams above show the corresponding spatial patterns. In particular, in the Helpman model, a monocentric distribution of the form $\boldsymbol{x} = (m_2, m_1, m_2, m_3)$ with $m_1 > m_2 > m_3$ is the stable equilibrium for $\phi \in (0, \phi^*)$. It converges to the full dispersion at ϕ^*, which is consistent with Proposition 1 (a).

As a further numerical example, Figure 10 shows the typical evolution of spatial patterns, assuming $N = 16$. We consider a monotonic increase in ϕ (i.e., a monotonic decrease in transport costs), and follow a path of stable spatial equilibria.

[21] For example, Kucheryavyy et al. (2024) focused on a specific but flexible two-region model that encompasses Allen and Arkolakis (2014) and Krugman (1991) as special cases. They essentially showed that the agricultural sector à la Krugman (1991) produces a global dispersion force that stabilizes the symmetric equilibrium at high transport costs, which is consistent with our results.

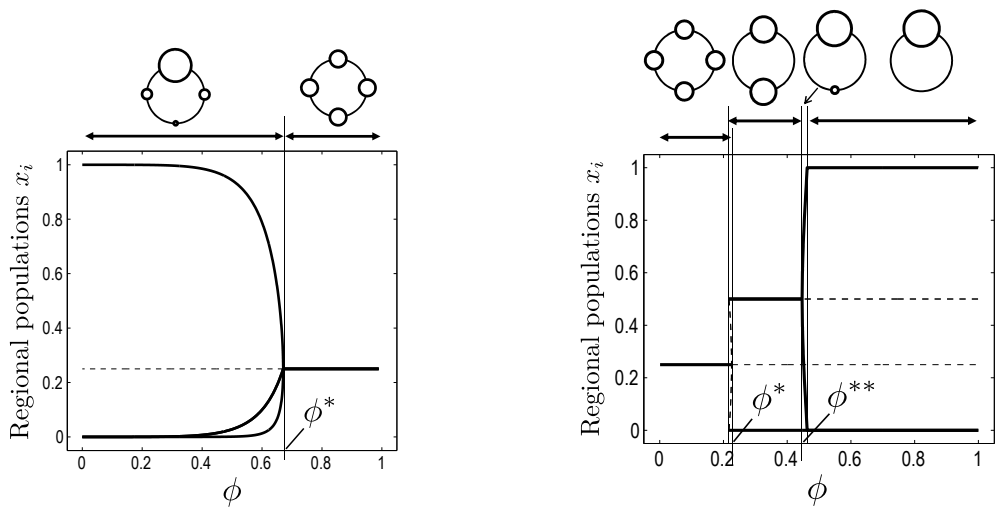

(A) The Helpman model (Type L)

(B) The Forslid–Ottaviano model (Type G)

Figure 9: Numerical illustration of Propositions 2 and 3.

Figure 10A considers the Type L model by Helpman (1998). The symmetric equilibrium $\bar{\boldsymbol{x}}$ is unstable if ϕ is small and the agents concentrate around a single peak. As ϕ increases, the monotonic spread of the single-peaked distribution occurs. At a critical level of ϕ, the spatial distribution converges to $\bar{\boldsymbol{x}}$ [Proposition 1 (a)]. In particular, stable equilibria are single-peaked throughout the process.

Figure 10B considers the Type G model of Krugman (1991). When ϕ is low, the symmetric equilibrium is stable. As ϕ increases, an endogenous transition occurs, and a polycentric equilibrium with eight agglomerations becomes stable [cf. Proposition 1 (b)]. Further increase in ϕ triggers successive instabilities: the number of agglomerations falls, the spacing between them widens, and each remaining center grows larger (cf. Proposition 3). As a result, the number of centers in the stable equilibrium evolves as $16 \to 8 \to 4 \to 2 \to 1$. In Type G models, spatial adjustment generates both winners and losers. Centers that initially grow may later decline as larger agglomerations expand at their expense. For instance, in Fig. 10B, the fifth region from the left initially gains population as ϕ increases but eventually loses population.

Figure 10C considers a many-region version of the Type LG model by Pflüger and Südekum (2008). The symmetric equilibrium is stable if ϕ is small. As ϕ increases, eight-centric agglomerations emerge at some point, as in Type G. Multiple bell-shaped agglomerations are generated at moderate ϕ. Increasing ϕ further causes a decrease in the number of agglomerations and the spread of each agglomeration. When ϕ is close to one, the economy becomes monocentric, as in Type L. Notably, in the large ϕ regime, the model exhibits a transformation from a two-peaked to a single-peaked pattern accompanied by local spreading. This broadly resembles the dual evolution of

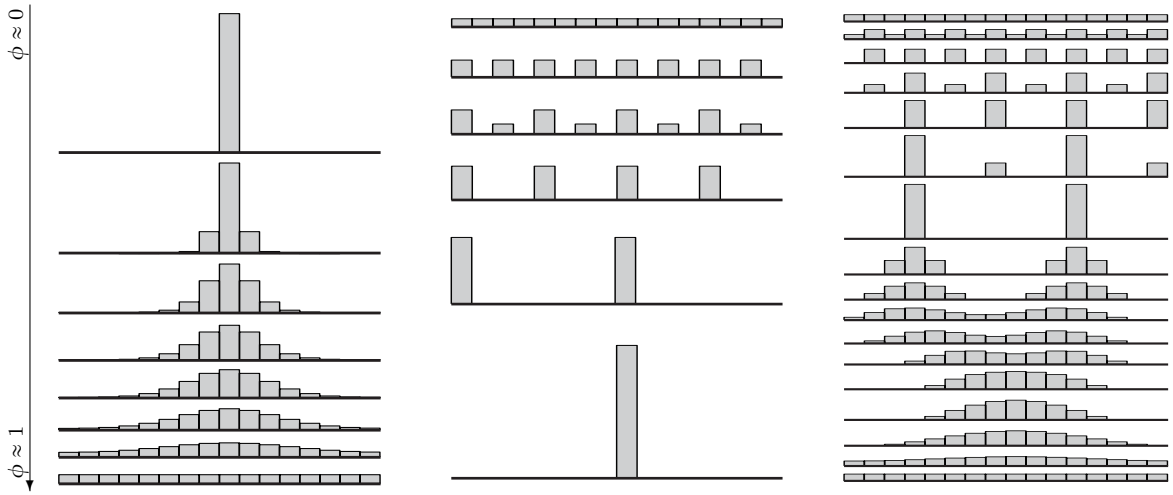

(A) Type L (B) Type G (C) Type LG

Figure 10: Stable spatial patterns at different transport cost levels.

Note: The spatial distributions in the circular economy are visualized as if it is on a line segment. In each figure, the leftmost region is neighboring to the rightmost one under Assumption C.

cities discussed in Section 1.[22]

4 Asymmetries

Real-world geography differs substantially from the stylized benchmarks discussed so far. Geographic accessibility and other region-fixed attributes can vary between locations, generating distortions absent in idealized settings. Yet, as a brief exploration in this section demonstrates, these exogenous asymmetries do not alter the core insights: the spatial scale of dominant dispersion mechanisms can fundamentally shape the spatial distribution and their response to transport costs.

4.1 Geographic accessibility

Asymmetries can arise solely from the underlying distance structure between regions. To illustrate this point, Figure 11 considers a square geography with homogeneous local fundamentals and compares stable equilibria under the Type L and Type G models. Unlike in a circular economy, some regions are "central" and therefore enjoy an inherent accessibility advantage. Nonetheless, our theoretical result continues to hold: the spatial distribution is monocentric under Type L, whereas it is polycentric under

[22]While the real-world dynamics appear to unfold simultaneously, the model generates these changes somewhat sequentially: first through a reduction in the number of peaks, and then through the flattening of the remaining agglomeration. This discrepancy may reflect limitations of the model, the most fundamental issues being the absence of inter-location commuting and dynamic decisions.

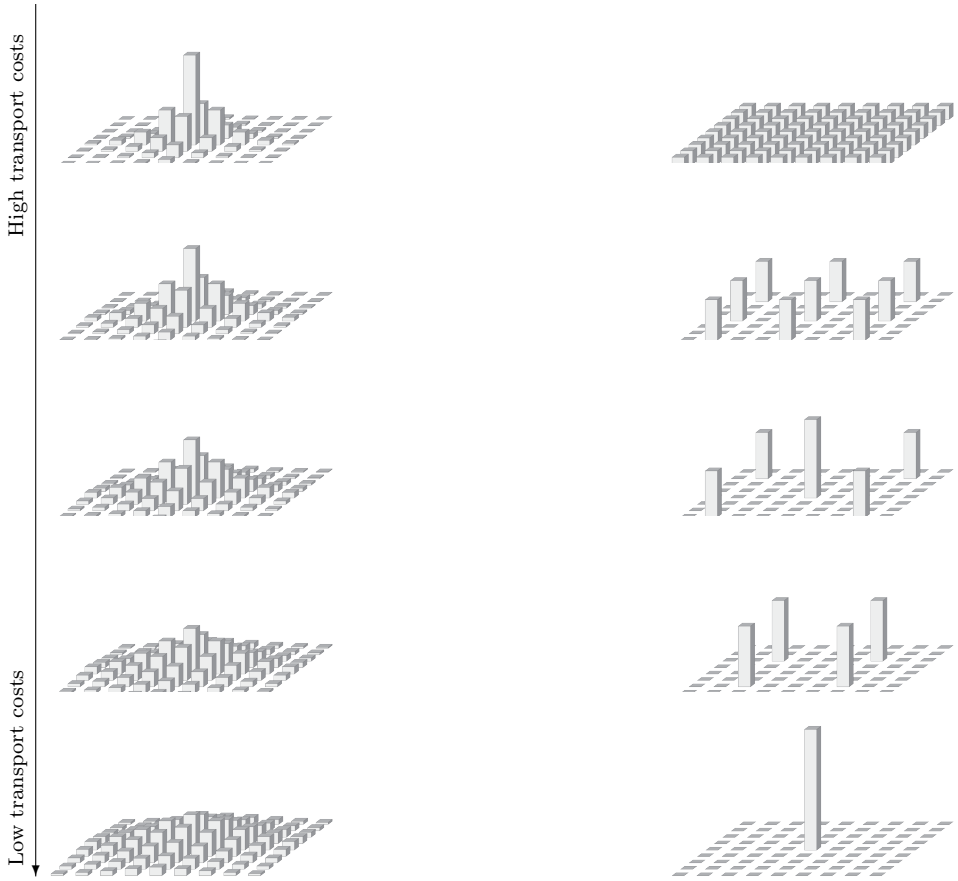

(A) The Allen–Arkolakis model (Type L) (B) The Krugman model (Type G)

Figure 11: Stable spatial patterns in a square economy ($9 \times 9 = 81$ locations).

Type G. Moreover, comparative statics with respect to reductions in transport costs are qualitatively similar to those in Figs. 10A and 10B: under Type L, population spreads monotonically, while under Type G, agglomeration proceeds through successive concentration into fewer locations. See Appendix D for further examples. To obtain formal results for such asymmetric settings, one approach is to select tractable models representative of each type and study their implications across alternative network structures, following the strategy of Matsuyama (2017) in a trade context.

4.2 Local fundamentals

Other than innate accessibility advantages, region-specific parameters such as exogenous productivity and amenity levels are equally fundamental, especially in quantitative spatial models (QSMs). For example, in the model of Allen and Arkolakis (2014), indirect utility can be written as

$$v_i(\boldsymbol{x}) = (u_i x_i^{-\beta}) \cdot \Big(\sum_{k \in \mathcal{I}} w_k^{1-\sigma} \left(b_k x_k^{\alpha}\right)^{\sigma-1} \phi_{ki} \Big)^{1/(\sigma-1)} w_i \tag{39}$$

where $u_i x_i^{-\beta}$ captures congestion in local amenities, with u_i denoting a region-specific amenity parameter. The nominal wage w_i is determined in market equilibrium given the population distribution $\boldsymbol{x}$ and satisfies

$$w_i x_i = \sum_{j \in \mathcal{I}} \frac{w_i^{1-\sigma} \left(b_i x_i^{\alpha}\right)^{\sigma-1} \phi_{ij}}{\sum_{k \in \mathcal{I}} w_k^{1-\sigma} \left(b_k x_k^{\alpha}\right)^{\sigma-1} \phi_{kj}} w_j x_j \qquad \forall i \in \mathcal{I}, \tag{40}$$

where $b_i x_i^{\alpha}$ represents within-region productivity spillovers driven by local population size, and b_i is a region-specific productivity parameter.

The key elasticities are $\alpha > 0$, $\beta > 0$, and $\sigma > 1$. The equilibrium is unique if $\alpha - \beta < 0$. In this case, given the observed population vector $\hat{\boldsymbol{x}}$, we can uniquely solve for the region-specific parameters $\{u_i\}$ and $\{b_i\}$ that rationalize $\hat{\boldsymbol{x}}$ as the model's equilibrium. A natural question then is how such regional differences affect our results.

To address this question, the stylized circular economy remains useful. Consider a spatial model with the proximity structure described in Assumption C, allowing for region-specific amenities $\boldsymbol{a} = (a_i)_{i \in \mathcal{I}}$ with $a_i > 0$. When $a_i = \bar{a}$ for all i, we recover the symmetric circular economy of Section 3, for which $\bar{\boldsymbol{x}}$ is an equilibrium. If we slightly perturb $\boldsymbol{a}$ from the symmetric case $\bar{\boldsymbol{a}} \equiv (\bar{a}, \bar{a}, \ldots, \bar{a})$, then $\bar{\boldsymbol{x}}$ is also slightly perturbed to form a new equilibrium $\boldsymbol{x}(\boldsymbol{a})$. Importantly, this mapping $\boldsymbol{x}(\boldsymbol{a})$ depends on the specification of the indirect utility function $\boldsymbol{v}$.

Given $\boldsymbol{x}(\boldsymbol{a})$, to summarize the overall effect of heterogeneities in $\boldsymbol{a}$ on the spatial distribution, we can use the covariance between each region's relative advantage and its deviation in population share from $\bar{\boldsymbol{x}}$:

$$\rho \equiv \sum_{i \in \mathcal{I}} \overbrace{(a_i - \bar{a})}^{\text{Exogenous regional (dis)advantage}} \underbrace{(x_i(\boldsymbol{a}) - \bar{x})}_{\text{Endogenous deviation from } \bar{\boldsymbol{x}}}. \tag{41}$$

If $\rho = 0$, variations in $\boldsymbol{a}$ have no effect on the equilibrium spatial distribution. Without loss of generality, we focus on the case $\rho > 0$, where regions with higher amenities tend to attract a larger population share.

Since the mapping $\boldsymbol{x}(\boldsymbol{a})$ is model dependent, the magnitude of ρ for a given transport cost level captures how strongly a model's endogenous forces translate variation in $\boldsymbol{a}$ into variation in regional population shares. Then, how ρ responds to transport cost changes provides a convenient summary statistic of model behavior. Propositions 4 and 5 in Online Appendix E formally shows that the sensitivity of ρ to transport costs differs markedly across models, reflecting differences in the spatial scale at which dispersion forces operate. Specifically, in models with pronounced global dispersion

forces, improved interregional access tends to *magnify* initial local advantages: ρ increases as the freeness of transport ϕ increases and the population becomes more concentrated in the regions favored due to exogenous advantages. By contrast, in models with strong local dispersion forces, the same transport improvement tends to *dampen* the role of innate heterogeneity, resulting in a flatter distribution, and ρ decreases as ϕ increases. These patterns are consistent with the two-region examples in Figs. 4C and 4D.

4.3 The combination: A quantitative example

In reality, both geographic accessibility and local fundamentals vary across regions. In this context, Sugimoto et al. (2025) provide a quantitative investigation of how spatial models behave when these two sources of heterogeneity interact, documenting important qualitative differences in counterfactual predictions across QSMs. They develop a Type LG model to evaluate how shocks to transport accessibility reshape the spatial distribution of economic activity in Japan, and contrast its predictions with those of a Type L model based on Helpman (1998). The Type LG model builds on the Helpman framework but extends it by introducing multiple production factors with different degrees of mobility: labor is freely mobile across regions, land is immobile, and intermediate inputs are tradable subject to transport costs. Workers choose locations based on indirect utility that depends on wages, prices for tradable goods, land rents, and region-fixed amenities. Although Sugimoto et al. (2025) do not assume immobile workers, incorporating land as an immobile production input gives rise to a global dispersion force, as discussed in Pflüger and Tabuchi (2010).

Sugimoto et al. (2025) discipline the models using Japanese data for 2005, covering 432 regional units defined primarily by Urban Employment Areas (Kanemoto and Tokuoka, 2002). Transport costs are estimated in a two-stage procedure following Allen and Arkolakis (2014), using information on the multimodal transport network (road, rail, air, and sea). Other key parameters, such as elasticities and factor shares, are taken from existing estimates. For each model, region-fixed amenities are calibrated to match the observed population distribution under a unique-equilibrium assumption, and the calibrated models are used to evaluate the counterfactual effects of removing the highway network.

For comparison, Figure 12A shows the observed population changes from 1970 to 2020 (reported backward in time), highlighting the long-run shift toward major metropolitan centers such as Tokyo, Osaka, and Nagoya, a pattern associated with the sustained decline in transport costs.

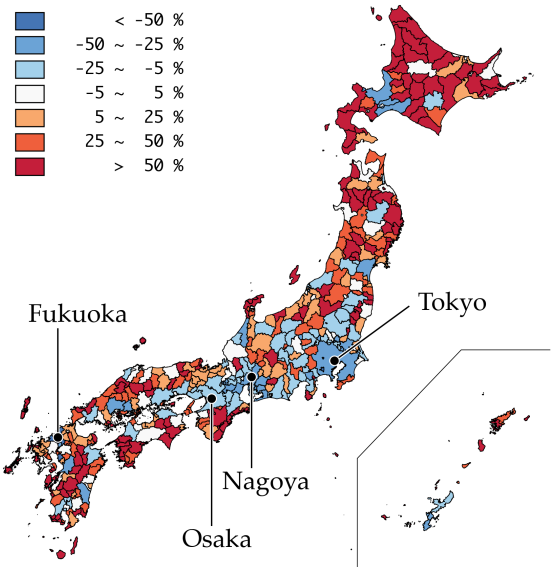

(A) Observed (from 2020 to 1970)

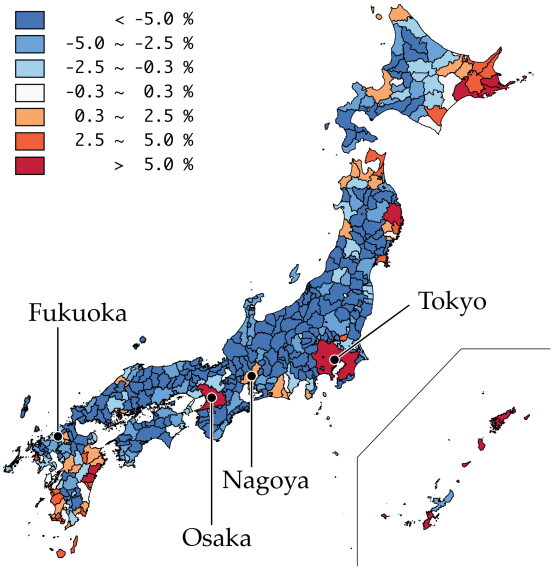

(B) Removal of highways (Type L)

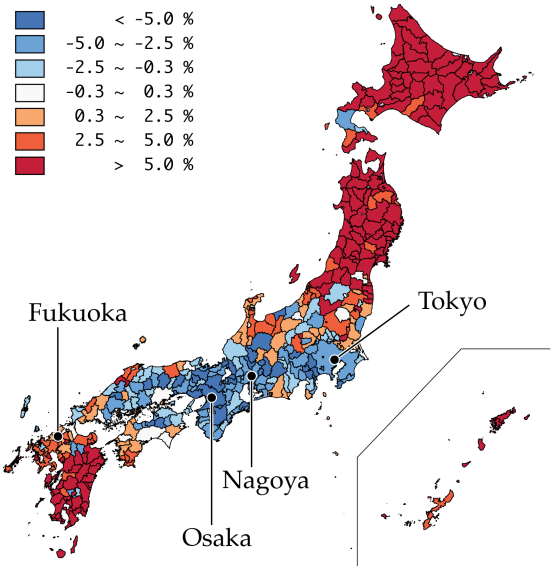

(C) Removal of highways (Type LG)

Figure 12: Observed and counterfactual population change rates of Japanese regions.

Note: Figures are constructed using the simulation results from Sugimoto et al. (2025). Panel (A) reports the observed (backward-looking) growth ratio, $(x_i^{1970} - x_i^{2020})/x_i^{2020} \times 100$ (%). Panel (B) shows the counterfactual growth ratio, $(x_i^{\text{Counterfactual}} - x_i^{2005})/x_i^{2005} \times 100$ (%), for a multi-region extension of Helpman (1998). Panel (C) presents the counterfactual growth ratio generated by the new model developed in Sugimoto et al. (2025).

Figures 12B and 12C present counterfactual simulations based on calibrated Type L and Type LG models, respectively, revealing a sharp contrast across the two frameworks. In the Type L model, highway removal induces further population concentration in core regions (Fig. 12B), consistent with the theoretical prediction that higher transport costs reinforce agglomeration. By contrast, the same shock in the Type LG model generates a substantial population shift toward peripheral regions (Fig. 12C),

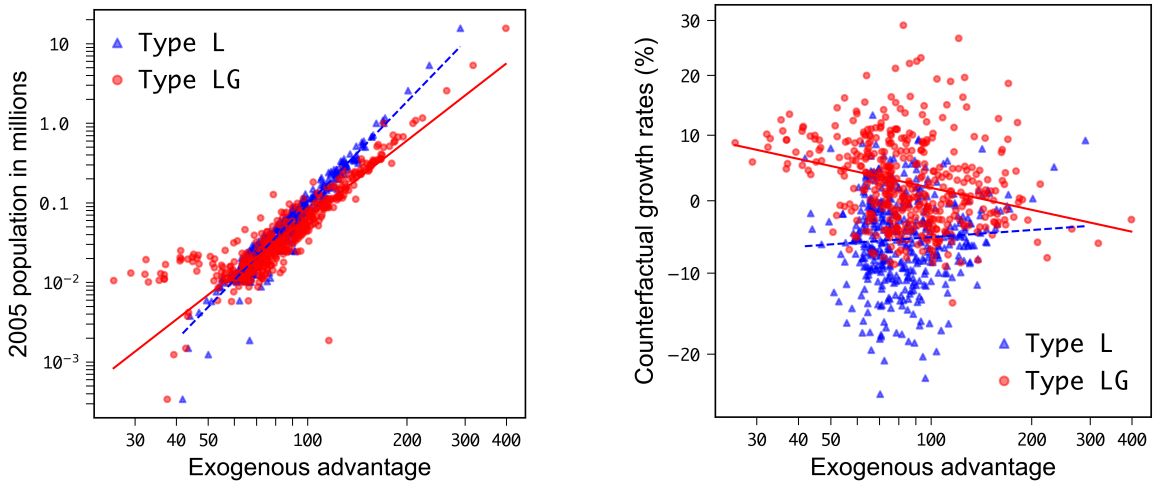

(A) Calibration to the population in 2005

(B) Counterfactual growths

Figure 13: Comparison of model behaviors in Fig. 12

Note: Panel (A): In both models, beyond 90% of log population variation is explained by exogenous region-fixed fundamentals (a composite of observed land area and unobserved amenities). Panel (B): In the Helpman model (Type L), growth rates and exogenous fundamentals are positively associated, i.e., highway removal induces growths at high-amenity regions, which are, as Panel (A) shows, essentially more populated regions in 2005. The converse holds true for Sugimoto et al.'s Type LG model as we observe negative association between exogenous fundamentals and growth rates.

reflecting the global dispersion forces arising from immobile land in production.

Figure 13 summarizes how each model translates exogenous regional advantages into equilibrium population responses. Panel (A) shows that, in both models, more than 90% of the variation in log population levels in 2005 is explained by exogenous region-fixed fundamentals, constructed as a composite of observed land area and calibrated amenities. Panel (B) relates these fundamentals to counterfactual growth rates following highway removal (an increase in transport costs). In the Type L model, growth rates are positively associated with exogenous advantages: regions with higher amenities, typically more populated regions in the baseline, experience relative population gains. In contrast, the Type LG model exhibits a negative association between fundamentals and growth rates, indicating that more advantaged core regions shrink relative to the periphery when transport costs rise.

These qualitative reversals demonstrate that the counterfactual implications of transport policies depend critically on the nature and spatial scale of the dispersion forces embedded in the QSM. Even when models fit the baseline population distribution equally well, their predictions can diverge sharply once policy counterfactuals are considered in asymmetric geographic settings.

4.4 On quantitative spatial models

The findings highlight a need to reconsider how endogenous economic forces are represented in QSMs. A central premise of the QSM literature is that it "does not aim to provide a fundamental explanation for the agglomeration of economic activity, but rather to provide an empirically relevant quantitative model to perform general equilibrium counterfactual policy exercises" (Redding and Rossi-Hansberg, 2017, p. 23). Building on this premise, QSMs typically impose equilibrium uniqueness and interpret unexplained interregional variation (i.e., structural residuals) as innate regional fundamentals. As a result, much of the observed variation is attributed to structural residuals (cf. Fig. 13A), and endogenous forces play a more limited role than in stylized theories of agglomeration.[23]

However, as the Japan example in Section 4.3 illustrates, seemingly innocuous choices regarding endogenous forces in QSMs can lead to markedly different counterfactual predictions, especially for distributional outcomes across regions. Most regional QSMs are Type L and rely on local dispersion forces for tractability (Redding, 2025b, Footnote. 8), which leads them to predict decentralization as transport costs fall.[24] This narrows the range of distributional outcomes such models can generate and, in turn, constrains the policy conclusions that can be drawn.

Further, some empirical contexts may be at odds with the unique-equilibrium assumption. For large transport projects such as highway systems, winners and losers may be uncertain ex-ante, making multiple equilibria potentially relevant. Evidence from the Chinese urban system indicates that urban hierarchies can be based on strong agglomeration forces or immobile factors (Baum-Snow et al., 2020), both of which can generate multiple equilibria. The persistence of spatial patterns further indicates that strong agglomeration forces and path dependence shape long-run regional outcomes (Lin and Rauch, 2022). A central challenge is therefore to assess whether incorporating such forces improves the empirical fit and counterfactual performance of QSMs. Relatedly, Graham and Hörcher (2024) argue that while QSMs hold promise for applied transport policy analysis, they are not yet practice-ready, citing model validation and uncertainty quantification as key obstacles. These challenges are closely tied to how endogenous forces are specified in QSMs, since the strength and nature of agglomeration and dispersion mechanisms critically determine equilibrium spatial structure and, ultimately, the robustness of counterfactual predictions.

[23] For example, in the seminal works of Redding and Sturm (2008) and Allen and Arkolakis (2014), structural residuals account for 90% and 78% of the logarithmic variation of the city size.

[24] A subtle point is that the local–global distinction reflects detailed modeling choices rather than broad economic mechanisms. For example, a "congestion" force can be global if it arises from crowding of facilities that are accessible across regions with positive transport costs.

5 Concluding remarks

We briefly discuss several examples to illustrate that our theoretical framework also offers a unifying interpretation of seemingly heterogeneous empirical findings. See Duranton and Turner (2025) for a more comprehensive survey of empirical evidence on how transport infrastructure affects urban and regional growth.

Evidence on regional growth from Faber (2014) is consistent with the predictions of Type G or GL models. He examines peripheral cities in China and finds negative effects on economic output. This may reflect a tendency for economic activity to concentrate in relatively larger or more central regions as transport access improves.[25] Baum-Snow et al. (2020) provide complementary evidence for China, documenting slower growth in the hinterland prefectures compared to regional primates following the expansion of the highway system.

In the intra-urban context, Baum-Snow (2007) and Baum-Snow et al. (2017) provide evidence for the US metropolitan areas from 1950 to 1990 and for Chinese prefectures from 1990 to 2010. Both studies examine how the share of population or production in the central area within a larger region changes as the transportation infrastructure expands, and both report negative effects in the central area. This is consistent with the behavior of Type L or LG models after transport investments. Such local spread can also be viewed as suburbanization driven by improved intra-urban transport infrastructure or by the diffusion of motorized transportation in the Alonso–Muth–Mills framework.[26]

As seen above, a unified theoretical framework can help synthesize and interpret empirical findings. Since this study focuses on static models with a single agent type, further scrutinies are essential for providing a bird's-eye view of both the empirical evidence and the now vast quantitative spatial economics literature. We conclude by outlining two directions that merit further theoretical investigation.

First, it is important to consider multiple types of mobile agents that differ in their proximity matrices and/or the degree of increasing returns they experience. Such heterogeneity is ubiquitous in multi-sector models (Fujita et al., 1999b; Hsu, 2012; Gaubert, 2018; Davis and Dingel, 2020) and in intracity models with multiple types of agents (e.g., Fujita and Ogawa, 1982; Lucas and Rossi-Hansberg, 2002; Ahlfeldt et al., 2015; Heblich et al., 2020). For example, Duranton et al. (2014) studied the impact of new highway connections on intercity trade in the US and showed that heavier industries are more sensitive to improved access. Allen et al. (2024) considered a quite general

[25] Duranton and Turner (2012) document that transport infrastructure in neighboring MSAs negatively affects the employment growth rate of an MSA (Table E2), a pattern consistent with global agglomeration.

[26] The structural transformation away from agriculture frees land around cities and also contributes to the decline of urban density (Coeurdacier et al., 2025). This can also be interpreted through the AMM framework as a reduction in the opportunity cost of land.

spatial model with multiple spatial interactions, but the characterization of endogenous equilibrium spatial structure has yet to be done, in particular for the cases with multiple equilibria. Circular geography provides a tractable starting point for analysis of many-locations under such structures (Tabuchi and Thisse, 2011; Osawa and Akamatsu, 2020). As Hsu (2012) suggests, the incorporation of sectoral heterogeneity can be particularly important for understanding the mechanisms behind the remarkable regularities in the size and spatial variation of cities (Mori et al., 2020).

Second, models with a continuum of agents as considered in this study are complementary to "granular" spatial models (e.g., Ahlfeldt et al., 2022), in which endogenous agglomeration arises from increasing returns and the indivisibility of agents. Continuum-agent models can replicate systematic spatial regularities, such as periodic agglomeration patterns and city-size distributions that include their fractal structure (e.g., Hsu, 2012; Tabuchi and Thisse, 2011; Mori et al., 2023). Granular spatial models are better suited to capture idiosyncratic location choices by superstar firms and large plants (e.g., Greenstone et al., 2010). Combining these two approaches may yield a deeper understanding of the spatial patterns of economic activities as the result of endogenous forces.

A Proofs

A.1 Proof of Lemma 1

We can represent Δ in terms of marginal migration from region 2 to 1: $\Delta(\epsilon) := \Delta(\bar{\boldsymbol{x}} + \frac{\epsilon}{2}(1,-1)) = v_1(\bar{x}+\frac{\epsilon}{2}, \bar{x}-\frac{\epsilon}{2}) - v_2(\bar{x}+\frac{\epsilon}{2}, \bar{x}-\frac{\epsilon}{2})$. Then, $\omega = \frac{\bar{x}}{\bar{v}}\Delta'(\epsilon)|_{\epsilon=0}$, meaning that ω is proportional to the directional derivative of Δ with respect to the unit migration from region 2 to 1, as $\frac{1}{2}(1,-1)$ is a normalized vector. Here, we used the fact that $\frac{\partial v_1}{\partial x_1}(\bar{\boldsymbol{x}}) = \frac{\partial v_2}{\partial x_2}(\bar{\boldsymbol{x}})$ and $\frac{\partial v_1}{\partial x_2}(\bar{\boldsymbol{x}}) = \frac{\partial v_2}{\partial x_1}(\bar{\boldsymbol{x}})$ due to the symmetry of the regions at $\bar{\boldsymbol{x}}$. The stability condition based on the sign of ω is valid for general $\boldsymbol{v}$ provided that $\bar{v} > 0$.

A.2 Proof of Lemma 2

Let $\delta v_i(\boldsymbol{z}) \equiv v_i(\bar{\boldsymbol{x}} + \boldsymbol{z}) - v_i(\bar{\boldsymbol{x}})$ be the utility difference in each region under deviation $\boldsymbol{z}$. The utility gain for a mover from region j to i is

$$\frac{\bar{x}}{\bar{v}}\left(\delta v_i(\boldsymbol{z}) - \delta v_j(\boldsymbol{z})\right). \tag{A.1}$$

By adding up the utility gains for all the migrants in the economy, the aggregate utility gain for migrants is measured by $\omega(\boldsymbol{z}) = \frac{\bar{x}}{\bar{v}}\sum_{i\in\mathcal{I}}\delta v_i(\boldsymbol{z})z_i = \frac{\bar{x}}{\bar{v}}\delta\boldsymbol{v}(\boldsymbol{z})^\top\boldsymbol{z}$, as there are z_i agents migrated to region i (if $z_i > 0$) or from region i (if $z_i < 0$), each experiencing utility difference $\delta v_i(\boldsymbol{z})$ at both their origin and destination. The first-order approximation shows $\delta\boldsymbol{v}(\boldsymbol{z}) \approx \boldsymbol{v}(\bar{\boldsymbol{x}}) + \nabla\boldsymbol{v}(\bar{\boldsymbol{x}})\boldsymbol{z} - \boldsymbol{v}(\bar{\boldsymbol{x}}) = \nabla\boldsymbol{v}(\bar{\boldsymbol{x}})\boldsymbol{z}$ and hence gives $\omega(\boldsymbol{z}) = \boldsymbol{z}^\top\mathbf{V}\boldsymbol{z}$.

It is noted that $\omega(\boldsymbol{z})$ must be considered subject to $\boldsymbol{z} \in T$, where $T \equiv \{\boldsymbol{z} \in \mathbb{R}^N \mid \sum_{i\in\mathcal{I}} z_i = 0\}$ is the set of all feasible deviations that preserves the total population. To avoid technicality, the main text do not mention the constraint $\boldsymbol{z}_k \in T$. This constraint excludes deviations of the form $\boldsymbol{z} = (\epsilon, \epsilon, \ldots, \epsilon)$, which represents the symmetric increase or decrease of population across all regions.

A.3 Proof of Proposition 1

We consider spatial models described by a *payoff function* (i.e., indirect utility) $\boldsymbol{v}(\boldsymbol{x}) \equiv (v_i(\boldsymbol{x}))_{i\in\mathcal{I}}$, parametrized by a proximity matrix $[\phi_{ij}]$, along with Assumption C. Let $\mathbf{D}$ be the row-normalized proximity matrix, whose (i,j)th element is $\frac{\phi_{ij}}{\sum_{k\in\mathcal{I}}\phi_{ik}}$. Throughout, we assume that $\boldsymbol{v}$ is differentiable if $x_i > 0$ for all $i \in \mathcal{I}$. The precise version of the symmetry of exogenous local fundamentals in Assumption C is the following:

Assumption S. For all $\boldsymbol{x}$, payoff function $\boldsymbol{v}$ satisfies $\boldsymbol{v}(\mathbf{P}\boldsymbol{x}) = \mathbf{P}\boldsymbol{v}(\boldsymbol{x})$ for all permutation matrices $\mathbf{P}$ that satisfy $\mathbf{PD} = \mathbf{DP}$. ■

Example 4. Suppose $N = 4$. If we consider regions 1 and 3, swapping their indices corresponds to applying the following permutation matrix to the spatial distribution and the payoff function:

$$\mathbf{P} = \begin{bmatrix} 0 & 0 & 1 & 0 \\ 0 & 1 & 0 & 0 \\ 1 & 0 & 0 & 0 \\ 0 & 0 & 0 & 1 \end{bmatrix}. \tag{A.2}$$

This matrix simply switches the values of x_1 and x_3 in any vector (x_1, x_2, x_3, x_4). That is, $\mathbf{P}\boldsymbol{x} = (x_3, x_2, x_1, x_4)$. This corresponds to relabeling the regions while keeping their physical positions fixed. The condition $\mathbf{PD} = \mathbf{DP}$ ensures that the relabeling preserves the spatial relationships encoded in $\mathbf{D}$. If $\boldsymbol{v}$ does not include any region-specific heterogeneities, then the transformed utility vector must satisfy $\boldsymbol{v}(\mathbf{P}\boldsymbol{x}) = \mathbf{P}\boldsymbol{v}(\boldsymbol{x})$. This property is called *equivariance*; it ensures that utility differences are determined entirely by the spatial distribution, not by arbitrary index labels. Equivariance allows us to employ the machineries from group-theoretic bifurcation theory (see, e.g., Golubitsky and Stewart, 2003; Golubitsky et al., 2012; Ikeda and Murota, 2014). ■

Under Assumption C, we can use the full dispersion as the initial state.

Lemma 3. Under Assumption C (including Assumption S), the uniform distribution of agents, $\bar{\boldsymbol{x}} = (\bar{x}, \bar{x}, \ldots, \bar{x})$ with $\bar{x} \equiv 1/N$, is a spatial equilibrium. ■

Proof. For any permutation matrix $\mathbf{P}$, $\bar{\boldsymbol{x}} = \mathbf{P}\bar{\boldsymbol{x}}$. Then, $\boldsymbol{v}(\mathbf{P}\bar{\boldsymbol{x}}) = \mathbf{P}\boldsymbol{v}(\bar{\boldsymbol{x}})$ reduces to $\boldsymbol{v}(\bar{\boldsymbol{x}}) = \mathbf{P}\boldsymbol{v}(\bar{\boldsymbol{x}})$ for all permutation matrix $\mathbf{P}$ that satisfies $\mathbf{PD} = \mathbf{DP}$. This implies that $v_i(\bar{\boldsymbol{x}}) = v_j(\bar{\boldsymbol{x}})$ for any $i, j \in \mathcal{I}$. That is, $\bar{\boldsymbol{x}}$ is a spatial equilibrium. □

We focus on a class of models that include all models discussed in the main text. As in the main text, let $\mathbf{V} = \frac{\bar{x}}{\bar{v}} \nabla \boldsymbol{v}(\bar{\boldsymbol{x}})$ be the *benefit matrix* for a given payoff function.

Definition 2. A *canonical model* is a model associated with a rational function Ω that is continuous over $[0, 1]$ such that $\mathbf{V} = \Omega(\mathbf{D})$. We call Ω the *gain function* of the model.

In Definition 2, a rational function Ω is a function of form $\Omega(\cdot) = \Omega^\sharp(\cdot)/\Omega^\flat(\cdot)$ with polynomials $\Omega^\sharp(\cdot)$ and $\Omega^\flat(\cdot) \neq 0$, where our convention is that $\Omega^\flat(\cdot) > 0$. Given such Ω, we let $\Omega(\mathbf{D}) = \Omega^\flat(\mathbf{D})^{-1}\Omega^\sharp(\mathbf{D})$, where, for a polynomial $P(\Theta) = c_0 + c_1\Theta + c_2\Theta^2 + \cdots$, we define $P(\mathbf{D}) = c_0\mathbf{I} + c_1\mathbf{D} + c_2\mathbf{D}^2 + \cdots$, with $\mathbf{I}$ being the identity matrix.

Below, we study the stability of $\bar{\boldsymbol{x}}$ in canonical models. Formally, we must introduce some dynamics to define the stability of $\bar{\boldsymbol{x}}$ and study agglomeration from there. For a wide class of dynamics, however, we can focus on the analysis of the benefit matrix $\mathbf{V}$.

Lemma 4. Assume a canonical model and assume Assumption C. For a wide class of myopic adjustment dynamics, $\bar{\boldsymbol{x}}$ is stable (unstable) if the largest eigenvalue of $\mathbf{V}$, excluding the one corresponding to $\mathbf{1} = (1, 1, \ldots, 1)$, is smaller (greater) than zero. Furthermore, if only the sign of the largest eigenvalue turns from negative to positive at some $\phi^* \in (0, 1)$, then a new spatial equilibrium branches from $\bar{\boldsymbol{x}}$ at ϕ^*, toward the direction of associated eigenvector. ■

Proof. See Section A.4. □

We can assume, for example, the replicator dynamics (Taylor and Jonker, 1978) to define local stability of spatial equilibria (see the proof of Lemma 4 for more examples).

Thus, we only need the eigenvalues of $\mathbf{V}$. A useful fact is that, if $\{(\Theta_k, \boldsymbol{z}_k)\}$ are the eigenpairs (eigenvalue–eigenvector pairs) of the normalized proximity matrix $\mathbf{D}$, then the eigenpairs of $\mathbf{V} = \Omega(\mathbf{D})$ are given by $\{(\Omega(\Theta_k), \boldsymbol{z}_k)\}$ (e.g., Horn and Johnson, 2012, Section 1.1). Thus, we need the eigenpairs of $\mathbf{D}$. For the sake of simplicity, we assume that N is a multiple of four. Then, we have the following lemma.

Lemma 5 (Corollary of Akamatsu et al. (2012), Lemma 4.2)**.** Assume Assumption C. The largest eigenvalue of $\mathbf{D}$ is $\Theta_0 \equiv 1$, with $\boldsymbol{z}_0 = (1, 1, \ldots, 1)$ being the associated eigenvector. Including Θ_0, there are $\frac{N}{2} + 1$ distinct eigenvalues. Every eigenvalue Θ_k ($k \neq 0$) is a strictly decreasing function of ϕ, with $\lim_{\phi \downarrow 0} \Theta_k = 1$ and $\lim_{\phi \uparrow 1} \Theta_k = 0$. Let $\Theta_{\max}$ denote the largest eigenvalue and $\Theta_{\min}$ denote the smallest eigenvalue of $\mathbf{D}$ excluding Θ_0, respectively. Further, assume that N is a multiple of four. Then,

$$\Theta_{\max} = \Theta_1 \equiv \frac{1-\phi}{1+\phi} \cdot \frac{1-\phi^2}{1-2\cos(\kappa)\phi+\phi^2} \cdot \frac{1+\phi^{N/2}}{1-\phi^{N/2}} \tag{A.3}$$

$$\Theta_{\min} = \Theta_{N/2} \equiv \left(\frac{1-\phi}{1+\phi}\right)^2 \tag{A.4}$$

at any ϕ, with $\kappa = \frac{2\pi}{N}$, and $\Theta_{\max} = \Theta_1$ has multiplicity two. For a vector $\boldsymbol{z}$, let $\langle z_i \rangle_{i=0}^{N-1} \equiv \frac{1}{\|\boldsymbol{z}\|}(z_i)_{i=0}^{N-1}$ denote its normalized version. Then, the eigenvector associated with $\Theta_{\max}$ is $\boldsymbol{z}_1^+ \equiv \langle \cos(\kappa i) \rangle_{i=0}^{N-1}$ and $\boldsymbol{z}_1^- \equiv \langle \sin(\kappa i) \rangle_{i=0}^{N-1}$, and that associated with $\Theta_{\min}$ is $\boldsymbol{z}_{N/2} \equiv \langle (-1)^i \rangle_{i=0}^{N-1} = \langle 1, -1, 1, -1, \ldots, 1, -1 \rangle$. ■

Since $\Theta_k \in (0, 1)$ for all relevant k and Ω is well-defined for all $[0, 1]$, the eigenpairs of $\mathbf{V} = \Omega(\mathbf{D})$ are in fact given by $\{(\Omega(\Theta_k), \boldsymbol{z}_k)\}$. Thus, with $\omega_k \equiv \Omega(\Theta_k)$, the symmetric equilibrium $\bar{\boldsymbol{x}}$ is stable if $\omega_k < 0$ for all k.

As discussed in Section 2, if agglomeration (dispersion) force of the model is too strong, $\Omega(\Theta) > 0$ ($\Omega(\Theta) < 0$) can happen for all Θ whereby $\bar{\boldsymbol{x}}$ is unstable (stable) for all ϕ. As we are interested in spatial agglomeration in the course of changing ϕ, we assume that $\bar{\boldsymbol{x}}$ can switch its stability depending on ϕ:

Assumption E (Endogenous agglomeration occurs)**.** The values of the model parameters are such that Ω switches its sign at least once in $(0,1)$. ■

Under Assumption E, we can define three prototypical classes of canonical models (see Fig. 5 in the main text for illustration).

Definition 3. Under Assumption E, a canonical model with gain function Ω is

(a) **Type L**, if there can be one and only one $\Theta^{**} \in (0,1)$ such that $\Omega(\Theta) < 0$ for $\Theta \in (0,\Theta^{**})$, $\Omega(\Theta^{**}) = 0$, and $\Omega(\Theta) > 0$ for $\Theta \in (\Theta^{**},1)$.

(b) **Type G**, if there can be one and only one root $\Theta^* \in (0,1)$ for Ω such that $\Omega(\Theta) > 0$ for $\Theta \in (0,\Theta^*)$, $\Omega(\Theta^*) = 0$, and $\Omega(\Theta) < 0$ for $\Theta \in (\Theta^*,1)$.

(c) **Type LG**, if there can be two $\Theta^*, \Theta^{**} \in (0,1)$ such that $\Omega(\Theta^*) = \Omega(\Theta^{**}) = 0$ and $\Theta^{**} < \Theta^*$, with $\Omega(\Theta) < 0$ for $\Theta \in (0,\Theta^{**}) \cup (\Theta^*,1)$ and $\Omega(\Theta) > 0$ for $\Theta \in (\Theta^{**},\Theta^*)$.

As discussed in the main text, the classification corresponds to the composition of the consequential dispersion forces in the model. We focus on the three model classes defined above and consider the destabilization of $\bar{\boldsymbol{x}}$. There can be a fourth class of models such that $\boldsymbol{x}$ is stable for medium levels of Θ but not for small or large Θ. However, we are not aware of any model that falls into this category.

As we consider canonical models, there is a rational function $\Omega(\cdot) = \Omega^\sharp(\cdot)/\Omega^\flat(\cdot)$ with some polynomials $\Omega^\sharp$ and $\Omega^\flat(\cdot) > 0$. That is, $\Omega^\sharp(\cdot)$ determines the sign of ω_k and thus governs the stability of $\bar{\boldsymbol{x}}$. We will focus on $\Omega^\sharp$ below, and let $\omega^\sharp \equiv \Omega^\sharp(\Theta_k)$ so that $\mathrm{sgn}[\omega_k] = \mathrm{sgn}[\omega_k^\sharp]$. Fig. A.1 schematically shows connections between $\{\omega_k^\sharp\}$, $\Omega^\sharp(\Theta)$, and $\{\Theta_k\}$ to help understanding the following arguments.

Type L. By definition, there is Θ^{**} such that $\Omega^\sharp(\Theta) < 0$ for all $\Theta \in (0,\Theta^{**})$, that $\Omega^\sharp(\Theta^{**}) = 0$, and that $\Omega^\sharp(\Theta^{**}) > 0$ for all $\Theta \in (\Theta^{**},1)$. Thus, $\bar{\boldsymbol{x}}$ is stable if and only if $\Theta_k \in (0,\Theta^{**})$, so that $\omega_k^\sharp = \Omega^\sharp(\Theta_k) < 0$, for all k, i.e., if $\Theta^{**} > \max_k \Theta_k = \Theta_1$. Thus, $\bar{\boldsymbol{x}}$ is stable for all $(\phi^*,1)$ where ϕ^{**} is the unique solution for $\Theta_1(\phi) = \Theta^{**}$. Because $\Omega^\sharp(\Theta) > 0$ for all $\Theta \in (\Theta^{**},1)$ and Θ_1 is strictly decreasing, $\bar{\boldsymbol{x}}$ is unstable for all $(0,\phi^{**})$.

Type G. By definition, there is Θ^* such that $\Omega^\sharp(\Theta) < 0$ for all $\Theta \in (\Theta^*,1)$, that $\Omega^\sharp(\Theta^*) = 0$, and that $\Omega^\sharp(\Theta) > 0$ for all $\Theta \in (0,\Theta^*)$. By Lemma 5, $\{\Theta_k(\phi)\}$ are strictly decreasing from 1. Thus, $\bar{\boldsymbol{x}}$ is stable if and only if $\Theta_k \in (\Theta^*,1)$, so that $\omega_k^\sharp = \Omega^\sharp(\Theta_k) < 0$, for all k, i.e., if $\Theta^* < \min_k \Theta_k = \Theta_{N/2}$. Thus, $\bar{\boldsymbol{x}}$ is stable for all $(0,\phi^*)$ where $\phi^* = (1-\sqrt{\Theta^*})/(1+\sqrt{\Theta^*})$ is the unique solution for $\Theta_{N/2} = \Theta^*$. Because

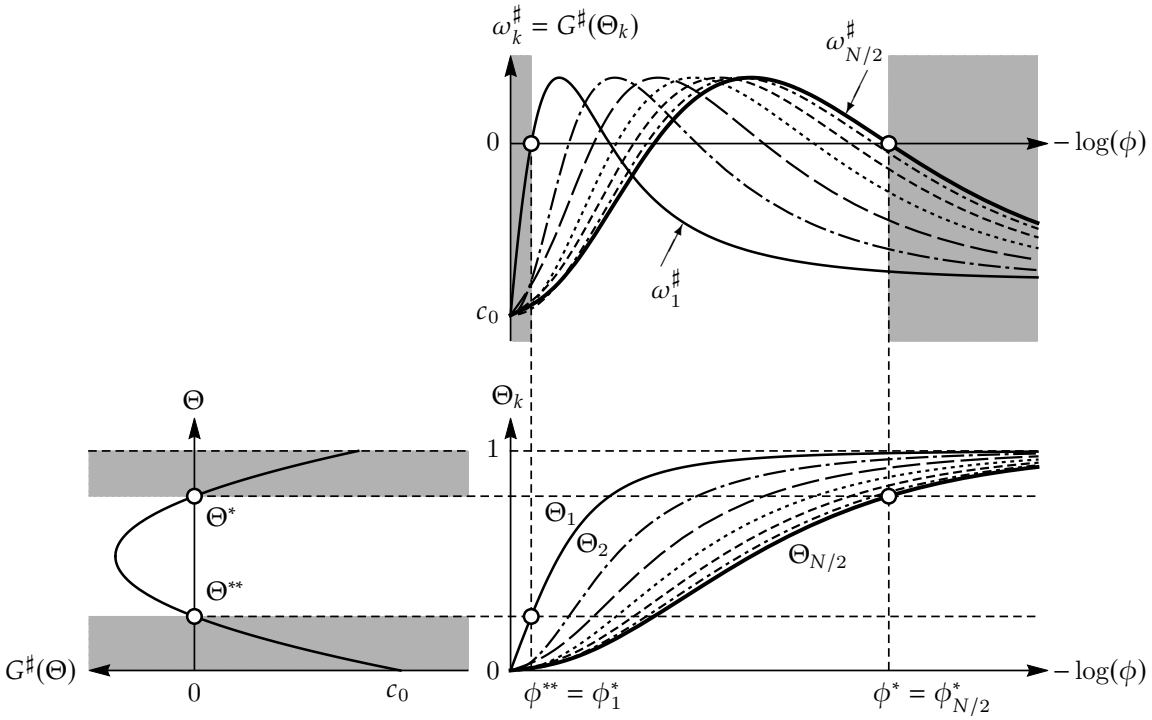

Figure A.1: The relationships between $\Omega^\sharp$, $\{\Theta_k\}$, and $\{\omega_k^\sharp\}$.

Note: Top: Graphs of $\omega_k^\sharp = \Omega^\sharp(\Theta_k)$. Bottom left: Net gain function $\Omega^\sharp$ for a hypothetical Type LG model with a quadratic net gain function of the form $\Omega^\sharp(\Theta) = c_0 + c_1\Theta + c_2\Theta^2$. Bottom right: The full set of eigenvalues $\{\Theta_k\}$ of $\mathbf{D}$. In the shaded regions of ϕ or Θ, $\bar{\boldsymbol{x}}$ is stable. For the ϕ axis, the negative log scale is used for better readability, with the transport cost level being high toward the right. We have $\max\{\Theta_k\} = \Theta_{\max}$ and $\min\{\Theta_k\} = \Theta_{\min}$ at any given level of ϕ.

$\Omega^\sharp(\Theta) > 0$ for all $\Theta \in (0, \Theta^*)$ and $\Theta_{N/2}$ is strictly decreasing, $\bar{\boldsymbol{x}}$ is unstable for all $(\phi^*, 1)$ because $\omega_{N/2}^\sharp > 0$ for the range.

Type LG. Via similar logic, we see $\bar{\boldsymbol{x}}$ is stable if $\phi \in (0, \phi_{N/2}^*) \cup (\phi_1^*, 1)$.

Spatial patterns. Consider a state where $\bar{\boldsymbol{x}}$ is stable. From Lemma 4, at ϕ^* in Types G or LG, a polycentric pattern with $N/2$ peaks branches from $\bar{\boldsymbol{x}}$, while at ϕ^{**} in Types L or LG, a monocentric configuration branches from $\bar{\boldsymbol{x}}$. □

Remark 1. The bifurcation towards the monocentric direction ($k = 1$) is a *double bifurcation*, where the associated eigenvalue ω_1 has multiplicity two, that is, there are two linearly independent eigenvectors. Migration patterns at this bifurcation take the form $c^+\boldsymbol{z}_1^+ + c^-\boldsymbol{z}_1^-$ for $c^+, c^- \in \mathbb{R}$. Under Assumption C, only $(c^+, c^-) = (c, 0)$ or (c, c) for some $c \in \mathbb{R}$ are admissible (Ikeda et al., 2012). The conclusion of Proposition 1 is not affected as both combinations yield monocentric configurations. ■

Remark 2. Although Definition 3 introduces three prototypical model classes, Type LG models sometimes span multiple classes depending on parametric restrictions (e.g.,

models by Pflüger and Tabuchi, 2010; Kucheryavyy et al., 2024). In such cases, the parameter space can be partitioned to map model behavior to the typology. Also, the definition of models often impose parametric restrictions that fix their class. In principle, flexible specifications would allow empirical identification of the class supported by data through parameter estimation. ■

Remark 3. In Lemma 5, we assume that N is a multiple of four to ensure $\min_k\{\Theta_k\} = \Theta_{\frac{N}{2}}$. This is inconsequential for the broad implication of Proposition 1 on spatial patterns. If N is an even, $\min_k\{\Theta_k\} = \min\{\Theta_{\frac{N}{2}-1}, \Theta_{\frac{N}{2}}\}$. If N is an odd, $\min_k\{\Theta_k\} = \min\{\Theta_{\lfloor\frac{N}{2}\rfloor}, \Theta_{\lfloor\frac{N}{2}\rfloor-1}\}$. Thus, $\min_k\{\Theta_k\}$ corresponds to a polycentric direction, except for the case $N = 2$ or 3 in which polycentric patterns cannot occur. ■

Remark 4. Beyond the local result of the proposition, Ikeda et al. (2012) characterized the possible equilibrium configurations and bifurcations in symmetric circular economy by group-theoretic analysis. Two formal predictions are worth mentioning.

First, no symmetry-breaking bifurcations can occur after the emergence of a single-peaked spatial pattern. For Type L models, the spatial configuration remains monocentric for the whole range of ϕ if the full dispersion is unstable (Figs. 9A and C.1)

The other prediction is that, if M same-sized agglomerations are equidistantly placed on a circle, a symmetry-breaking bifurcation may reduce their number to $K < M$, with K again dividing N and the agglomerations remaining equidistant.

Proposition 1 (a) implies that Type G models yield $\frac{N}{2}$ agglomerations, with further bifurcations of the form $\frac{N}{2} \to \frac{N}{4} \to \frac{N}{8} \to \cdots \to 2 \to 1$ expected if N is a power of two (Akamatsu et al., 2012; Ikeda et al., 2012; Osawa et al., 2017). For Type L, Takayama et al. (2020) confirmed the emergence of single-peaked or monocentric patterns in the (Murata and Thisse, 2005) model. Akamatsu et al. (2016) formally compares Forslid and Ottaviano (2003) (Type G) and Helpman (1998) (Type L). All available formal results in the literature corroborates with Proposition 1 and the numerical examples in this study. ■

A.4 Proof of Lemma 4

A myopic adjustment dynamic is a system of ordinary differential equations that describes the rate of change in the spatial distribution $\boldsymbol{x}$. Denote the dynamic that adjusts $\boldsymbol{x}$ over the set of all possible spatial distributions $\mathcal{X} \equiv \{\boldsymbol{x} \geq \mathbf{0} \mid \sum_{i\in\mathcal{I}} x_i = 1\}$ by $\dot{\boldsymbol{x}} = \boldsymbol{f}(\boldsymbol{x})$, where $\dot{\boldsymbol{x}}$ represents the time derivative satisfying $\sum_{i\in\mathcal{I}} \dot{x}_i = 0$ so that the total population is invariant. For example, $\boldsymbol{f}(\boldsymbol{x}) = \tilde{\boldsymbol{f}}(\boldsymbol{x}, \boldsymbol{v}(\boldsymbol{x}))$ where $\tilde{\boldsymbol{f}}$ maps each pair $(\boldsymbol{x}, \boldsymbol{v}(\boldsymbol{x}))$ of a state and its associated payoff to a motion vector $\dot{\boldsymbol{x}}$.

We require the following conditions on $\boldsymbol{f}$: (RS) $\boldsymbol{f}(\boldsymbol{x}) = \mathbf{0}$ if $\boldsymbol{x}$ is a spatial distribution in which all populated regions earn the same payoff level, i.e., $v_j(\boldsymbol{x}^*) = v_k(\boldsymbol{x}^*)$ for all $j, k \in \{i \in \mathcal{I} \mid x_i^* > 0\}$, (PC) $\boldsymbol{v}(\boldsymbol{x})^\top \boldsymbol{f}(\boldsymbol{x}) > 0$ if $\boldsymbol{f}(\boldsymbol{x}) \neq \mathbf{0}$, and (Sym) $\mathbf{P}\boldsymbol{f}(\boldsymbol{x}) = \boldsymbol{f}(\mathbf{P}\boldsymbol{x})$ for *all* permutation matrices $\mathbf{P}$. We call dynamics that satisfy (RS), (PC), and (Sym) *admissible dynamics*. The conditions (RS) and (PC) are called *restricted stationality* and *positive correlation*, respectively (Sandholm, 2010). Also, (Sym) requires that $\boldsymbol{f}$ treats all regions symmetrically. Finally, we assume that $\boldsymbol{f}$ admits a C^1 extension to an open neighborhood of $\mathcal{X}$ in $\mathbb{R}^N$ to use simple derivatives.

Admissible dynamics include the Brown–von Neumann–Nash dynamic (Brown and von Neumann, 1950; Nash, 1951), the Smith dynamic (Smith, 1984), and Riemannian game dynamics (Mertikopoulos and Sandholm, 2018). The projection dynamic (Dupuis and Nagurney, 1993) and the replicator dynamic (Taylor and Jonker, 1978) are representative instances of Riemannian game dynamics that satisfy (Sym), and are often applied for regional models.

For the uniform distribution $\bar{\boldsymbol{x}}$, (RS) implies $\boldsymbol{f}(\bar{\boldsymbol{x}}) = \mathbf{0}$, i.e., $\bar{\boldsymbol{x}}$ is a stationary point of $\boldsymbol{f}$. Denote the Jacobian matrix of $\boldsymbol{f}$ at $\bar{\boldsymbol{x}}$ by $\mathbf{F} = [\frac{\partial f_i}{\partial x_j}(\bar{\boldsymbol{x}})]$. Assume that $\mathbf{F}$ has no eigenvalues with zero real parts. Then, $\bar{\boldsymbol{x}}$ is *linearly stable* if all the eigenvalues of $\mathbf{F}$, which we denote by $\{\eta_k\}$, have negative real parts, and *linearly unstable* if some eigenvalue has positive real parts (see,e.g., Hirsch et al., 2012). Spatial equilibrium $\bar{\boldsymbol{x}}$ is said to be *stable* (*unstable*) if it is linearly stable (unstable) under admissible dynamics. The marginal case in which the largest eigenvalue has zero real parts is unimportant as it often corresponds to measure-zero subsets of the parameter space.

Under admissible dynamics, the stability of $\bar{\boldsymbol{x}}$ can be determined by $\mathbf{V}$, i.e., without checking $\mathbf{F}$ explicitly. To exclude degenerate cases, assume that there is no other equilibrium in the neighborhood of $\bar{\boldsymbol{x}}$. Then, (PC) implies that there is a neighborhood $\mathcal{O} \subset \mathcal{X}$ of $\bar{\boldsymbol{x}}$ such that $\boldsymbol{v}(\boldsymbol{x})^\top \boldsymbol{f}(\boldsymbol{x}) > 0$ for all $\boldsymbol{x} \in \mathcal{O} \setminus \{\bar{\boldsymbol{x}}\}$. For small deviation $\boldsymbol{z} = \boldsymbol{x} - \bar{\boldsymbol{x}}$ with $\boldsymbol{x} \in \mathcal{O} \setminus \{\bar{\boldsymbol{x}}\}$, $\boldsymbol{f}(\boldsymbol{x}) \approx \boldsymbol{f}(\bar{\boldsymbol{x}}) + \nabla \boldsymbol{f}(\bar{\boldsymbol{x}})\boldsymbol{z} = \mathbf{F}\boldsymbol{z}$, $\boldsymbol{v}(\boldsymbol{x}) \approx \boldsymbol{v}(\bar{\boldsymbol{x}}) + \nabla \boldsymbol{v}(\bar{\boldsymbol{x}})\boldsymbol{z} = \bar{v}\mathbf{1} + \frac{\bar{v}}{\bar{x}}\mathbf{V}$, and $0 = \mathbf{1}^\top \dot{\boldsymbol{x}} = \mathbf{1}^\top \boldsymbol{f}(\boldsymbol{x}) \approx \mathbf{1}^\top \mathbf{F}\boldsymbol{z}$. Combined together, for all $\boldsymbol{x} \in \mathcal{O} \setminus \{\bar{\boldsymbol{x}}\}$,

$$\boldsymbol{v}(\boldsymbol{x})^\top \boldsymbol{f}(\boldsymbol{x}) \approx \left(\boldsymbol{v}(\bar{\boldsymbol{x}}) + \nabla \boldsymbol{v}(\bar{\boldsymbol{x}})\boldsymbol{z}\right)^\top \left(\boldsymbol{f}(\bar{\boldsymbol{x}}) + \mathbf{F}\boldsymbol{z}\right) = \tfrac{\bar{v}}{\bar{x}} \left(\mathbf{V}\boldsymbol{z}\right)^\top \left(\mathbf{F}\boldsymbol{z}\right) > 0. \tag{A.5}$$

Under Assumption C, we can choose the same set of eigenvectors for $\mathbf{V}$ and $\mathbf{F}$ because they are both symmetric *circulant* matrices. Let $\{\boldsymbol{z}_k\}$ be the set of eigenvectors and let ω_k and η_k be the eigenvalues of $\mathbf{V}$ and $\mathbf{F}$ associated with $\boldsymbol{z}_k$, respectively. Then, for each eigenvector $\boldsymbol{z}_k$ except for $\boldsymbol{z}_0 = \mathbf{1}$, Eq. (A.5) yields

$$\left(\mathbf{V}\boldsymbol{z}_k\right)^\top \left(\mathbf{F}\boldsymbol{z}_k\right) = \omega_k \eta_k > 0. \tag{A.6}$$

As $\mathbf{F}$ and $\mathbf{V}$ are both symmetric, η_k and ω_k are both real. Thus, Eq. (A.6) implies $\text{sgn}[\eta_k] = \text{sgn}[\omega_k]$. Therefore, $\bar{\boldsymbol{x}}$ is stable under all admissible dynamics if and only if $\omega_k < 0$ for *all* k, excluding $k = 0$ that corresponds to $\boldsymbol{z}_0 = \mathbf{1}$. Likewise, $\bar{\boldsymbol{x}}$ is unstable if and only if $\omega_k > 0$ for *some* k, again excluding $k = 0$.

Suppose exactly one ω_k changes sign from negative to positive at ϕ_k^*. Then, from Eq. (A.6), the corresponding eigenvalue of the Jacobian matrix of any admissible dynamic at $\bar{\boldsymbol{x}}$ must also cross zero at ϕ_k^*. It is standard in bifurcation theory (see, e.g., Hirsch et al., 2012; Kuznetsov, 2004) that the system departs from $\bar{\boldsymbol{x}}$ along the direction of the associated eigenvector $\boldsymbol{z}_k$, as it is tangent to the "unstable manifold" at the bifurcation point.

* * *

Appendices B to F are provided as a separate online appendix.

References

Ahlfeldt, Gabriel M., Stephen J. Redding, Daniel M. Sturm, and Nikolaus Wolf, "The economics of density: Evidence from the Berlin Wall," *Econometrica*, 2015, *83* (6), 2127–2189.

_ , Thilo Albers, and Kristian Behrens, "A granular spatial model," 2022. CEPR Discussion paper No. 17126.

Akamatsu, Takashi, Tomoya Mori, and Yuki Takayama, "Agglomerations in a Multi-region Economy: Polycentric versus monocentric patterns," Discussion papers, Research Institute of Economy, Trade and Industry (RIETI) 2016.

_ , _ , Minoru Osawa, and Yuki Takayama, "Replication data for: Spatial scale of agglomeration and dispersion: Number, spacing, and the spatial extent of cities," *Journal of Urban Economics,* Mendeley Data, 2026. https://doi.org/10.17632/j6b7mcyv6c.1.

_ , Yuki Takayama, and Kiyohiro Ikeda, "Spatial discounting, Fourier, and racetrack economy: A recipe for the analysis of spatial agglomeration models," *Journal of Economic Dynamics and Control*, 2012, *99* (11), 32–52.

Allen, Treb and Costas Arkolakis, "Trade and the topography of the spatial economy," *The Quarterly Journal of Economics*, 2014, *129* (3), 1085–1140.

_ and _ , "Quantitative regional economics," in Dave Donaldson and Stephen J. Redding, eds., *Handbook of Regional and Urban Economics*, Vol. 6, Elsevier, 2025, pp. 1–72.

_ , _ , and Xiangliang Li, "On the equilibrium properties of spatial models," *American Economic Review: Insights*, 2024, *6* (4), 472–89.

Anas, Alex, "Discrete choice theory, information theory and the multinomial logit and gravity models," *Transportation Research Part B: Methodological*, 1983, *17* (1), 13–23.

_ and Ikki Kim, "General equilibrium models of polycentric urban land use with endogenous congestion and job agglomeration," *Journal of Urban Economics*, 1996, *40* (2), 232–256.

_ and Rong Xu, "Congestion, land use, and job dispersion: A general equilibrium model," *Journal of Urban Economics*, 1999, *45* (3), 451–473.

_ and Yu Liu, "A regional economy, land use, and transportation model (RELU-TRAN©): formulation, algorithm design, and testing," *Journal of Regional Science*, 2007, *47* (3), 415–455.

Anderson, Simon P., Andre de Palma, and Jacques François Thisse, *Discrete Choice Theory of Product Differentiation*, MIT Press, 1992.

Armington, Paul S., "A theory of demand for product distinguished by place of production," *International Monetary Fund Staff Papers*, 1969, *16* (1), 159–178.

Baldwin, Richard E., Rikard Forslid, Philippe Martin, Gianmarco I. P. Ottaviano, and Frederic Robert-Nicoud, *Economic Geography and Public Policy*, Princeton University Press, 2003.

Baum-Snow, Nathaniel, "Did highways cause suburbanization?," *The Quarterly Journal of Economics*, May 2007, *122* (2), 775–805.

_ , J. Vernon Henderson, Matthew A. Turner, Qinghua Zhang, and Loren Brandt, "Does investment in national highways help or hurt hinterland city growth?," *Journal of Urban Economics*, 2020, *115*, 103124.

_ , Loren Brandt, J. Vernon Henderson, Matthew A. Turner, and Qinghua Zhang, "Roads, railroads and decentralization of Chinese cities," *Review of Economics and Statistics*, 2017, *99* (3), 435–448.

Beckmann, Martin J., "Spatial equilibrium in the dispersed city," in Yorgos Papageorgiou, ed., *Mathematical Land Use Theory*, Lexington Book, 1976, pp. 117–125.

Behrens, Kristian and Yasusada Murata, "On quantitative spatial economic models," *Journal of Urban Economics*, 2021, *123*, 103348.

Braid, Ralph M., "Heterogeneous preferences and non-central agglomeration of firms," *Regional Science and Urban Economics*, 1988, *18* (1), 57–68.

Brakman, Steven, Harry Garretsen, and Charles Van Marrewijk, *An introduction to geographical and urban economics: A spiky world*, Cambridge University Press, 2019.

Brown, George W. and John von Neumann, "Solutions of games by differential equations," in Harold W. Kuhn and Albert W. Tucker, eds., *Contributions to the Theory of Games I*, Princeton University Press, 1950, pp. 73–80.

Coeurdacier, Nicolas, Florian Oswald, and Marc Teignier, "Structural Change, Land Use and Urban Expansion," *The Review of Economic Studies*, 2025, p. rdaf091.

Combes, Pierre-Philippe, Gilles Duranton, Laurent Gobillon, Clément Gorin, and Frédéric Robert-Nicoud, "Urbanisation and urban divergence: France 1760–2020," 2023. Unpublished manuscript.

Davis, Donald R. and Jonathan I. Dingel, "The comparative advantage of cities," *Journal of International Economics*, 2020, *123*, 1032–91.

Dupuis, Paul and Anna Nagurney, "Dynamical systems and variational inequalities," *Annals of Operations Research*, 1993, *44* (1), 7–42.

Duranton, Gilles and Matthew A. Turner, "Urban growth and transportation," *Review of Economic Studies*, 2012, *79* (4), 1407–1440.

_ and _ , "Transportation infrastructure and urban and regional development," 2025. Unpublished manuscript.

_ , Peter M. Morrow, and Matthew A. Turner, "Roads and trade: Evidence from the US," *Review of Economic Studies*, November 2014, *81* (2), 681–724.

Faber, Benjamin, "Trade integration, market size, and industrialization: Evidence from China's national trunk highway system," *Review of Economic Studies*, 2014, *81* (3), 1046–1070.

Forslid, Rikard and Gianmarco I. P. Ottaviano, "An analytically solvable core-periphery model," *Journal of Economic Geography*, 2003, *33* (3), 229–240.

Fujita, Masahisa and Hideaki Ogawa, "Multiple equilibria and structural transformation of non-monocentric urban configurations," *Regional Science and Urban Economics*, 1982, *12*, 161–196.

_ **and Jacques-François Thisse**, *Economics of Agglomeration: Cities, Industrial Location, and Regional Growth (Second Edition)*, Cambridge University Press, 2013.

_ **, Paul R. Krugman, and Anthony Venables**, *The Spatial Economy: Cities, Regions, and International Trade*, Princeton University Press, 1999.

_ **,** _ **, and Tomoya Mori**, "On the evolution of hierarchical urban systems," *European Economic Review*, February 1999, *43* (2), 209–251.

Gaubert, Cecile, "Firm sorting and agglomeration," *American Economic Review*, 2018, *108* (11), 3117–3153.

Golubitsky, Martin and Ian Stewart, *The Symmetry Perspective: From Equilibrium to Chaos in Phase Space and Physical Space*, Vol. 200, Springer Science & Business Media, 2003.

_ **,** _ **, and David G. Schaeffer**, *Singularities and Groups in Bifurcation Theory*, Vol. 2, Springer Science & Business Media, 2012.

Graham, Dan and Daniel Hörcher, "Transport appraisal and quantitative spatial economics: A review of theory, empirics, and transport applications," Technical Report 2024. The Department for Transport, UK.

Greenstone, Michael, Richard Hornbeck, and Enrico Moretti, "Identifying agglomeration spillovers: Evidence from winners and losers of large plant openings," *Journal of Political Economy*, 2010, *118* (3), 536–598.

Harris, Britton and Alan G. Wilson, "Equilibrium values and dynamics of attractiveness terms in production-constrained spatial-interaction models," *Environment and Planning A*, 1978, *10* (4), 371–388.

Heblich, Stephan, Stephen J Redding, and Daniel M. Sturm, "The making of the modern metropolis: Evidence from London," *The Quarterly Journal of Economics*, 2020, *135* (4), 2059–2133.

Helpman, Elhanan, "The size of regions," in David Pines, Efrainm Sadka, and Itzhak Zilcha, eds., *Topics in Public Economics: Theoretical and Applied Analysis*, Cambridge University Press, 1998, pp. 33–54.

Henderson, J. Vernon, "The sizes and types of cities," *American Economic Review*, 1974, *64* (4), 640–656.

Hirsch, Morris W., Stephen Smale, and Robert L. Devaney, *Differential Equations, Dynamical Systems, and an Introduction to Chaos*, Academic Press, 2012.

Horn, Roger A. and Charles R. Johnson, *Matrix Analysis (Second Edition)*, Cambridge University Press, 2012.

Hsu, Wen-Tai, "Central place theory and city size distribution," *The Economic Journal*, 2012, *122*, 903–932.

Hunt, John Douglas and David C. Simmonds, "Theory and application of an integrated land-use and transport modelling framework," *Environment and Planning B: Planning and Design*, 1993, *20* (2), 221–244.

Ikeda, Kiyohiro and Kazuo Murota, *Bifurcation Theory for Hexagonal Agglomeration in Economic Geography*, Springer, 2014.

_ **, Takashi Akamatsu, and Tatsuhito Kono**, "Spatial period-doubling agglomeration of a core–periphery model with a system of cities," *Journal of Economic Dynamics and Control*, 2012, *36* (5), 754–778.

Kanemoto, Yoshitsugu and Kazuyuki Tokuoka, "Proposal for the standards of metropolitan areas of Japan (in Japanese)," *Journal of Applied Regional Science*, 2002, *7*, 1–15.

Krugman, Paul R., "Increasing returns and economic geography," *Journal of Political Economy*, 1991, *99* (3), 483–499.

_ **and Anthony J. Venables**, "Globalization and the Inequality of Nations," *The Quarterly Journal of Economics*, 1995, *110* (4), 857–880.

Kucheryavyy, Konstantin, Gary Lyn, and Andrés Rodríguez-Clare, "Spatial equilibria: The case of two regions," *Journal of International Economics*, 2024, *152*, 104008.

Kuznetsov, Yuri A., *Elements of Applied Bifurcation Theory (3rd Eds.)*, Springer-Verlag, 2004.

Lin, Jeffrey and Ferdinand Rauch, "What future for history dependence in spatial economics?," *Regional Science and Urban Economics*, 2022, *94*, 103628.

Lucas, Robert E. and Esteban Rossi-Hansberg, "On the internal structure of cities," *Econometrica*, 2002, *70* (4), 1445–1476.

Matsuyama, Kiminori, "Geographical advantage: Home market effect in a multi-region world," *Research in Economics*, 2017, *71*, 740–758.

McFadden, Daniel, "Conditional Logit Analysis of Qualitative Choice Behavior," in P Zarembka, ed., *Frontiers in Econometrics*, Academic Press, New York, 1974, pp. 105–142.

_ , "Modelling the choice of residential location," in A. Karlqvist, L. Lundqvist, F. Snickars, and J. Weibull, eds., *Spatial Interaction Theory and Planning Models*, Amsterdam: North Holland, 1978, pp. 75–96.

_ , "Modelling the choice of residential location," *Transportation Research Record*, 1978, *673*, 72–77.

Mertikopoulos, Panayotis and William H. Sandholm, "Riemannian game dynamics," *Journal of Economic Theory*, 2018, *177*, 315–364.

Mori, Tomoya, Takashi Akamatsu, Yuki Takayama, and Minoru Osawa, "Origin of power laws and their spatial fractal structure for city-size distributions," 2023. arXiv:2207.05346.

_ **, Tony E. Smith, and Wen-Tai Hsu**, "Common power laws for cities and spatial fractal structures," *Proceedings of the National Academy of Sciences*, 2020, *117* (12), 6469–6475.

Murata, Yasusada, "Product diversity, taste heterogeneity, and geographic distribution of economic activities:: market vs. non-market interactions," *Journal of Urban Economics*, 2003, *53* (1), 126–144.

_ **and Jacques-François Thisse**, "A simple model of economic geography à la Helpman–Tabucbi," *Journal of Urban Economics*, 2005, *58* (1), 137–155.

Nash, John, "Non-cooperative games," *Annals of Mathematics*, 1951, *54* (2), 286–295.

Osawa, Minoru and Takashi Akamatsu, "Equilibrium refinement for a model of non-monocentric internal structures of cities: A potential game approach," *Journal of Economic Theory*, 2020, *187*, 105025.

_ **,** _ **, and Yuki Takayama**, "Harris and Wilson (1978) model revisited: The spatial period-doubling cascade in an urban retail model," *Journal of Regional Science*, 2017, *57* (3), 442–466.

Palma, André de, Victor Ginsburgh, Yorgos Y. Papageorgiou, and Jacques-François Thisse, "The principle of minimum differentiation holds under sufficient heterogeneity," *Econometrica*, 1985, pp. 767–781.

Papageorgiou, Yorgos Y. and Terrence R. Smith, "Agglomeration as local instability of spatially uniform steady-states," *Econometrica*, 1983, pp. 1109–1119.

Pflüger, Michael, "A simple, analytically solvable, Chamberlinian agglomeration model," *Regional Science and Urban Economics*, 2004, *34* (5), 565–573.

_ **and Jens Südekum**, "Integration, agglomeration and welfare," *Journal of Urban Economics*, March 2008, *63* (2), 544–566.

Pflüger, Michael and Takatoshi Tabuchi, "The size of regions with land use for production," *Regional Science and Urban Economics*, 2010, *40* (6), 481–489.

Puga, Diego, "The rise and fall of regional inequalities," *European Economic Review*, 1999, *43* (2), 303–334.

Redding, Stephen J., "Quantitative urban economics," in Dave Donaldson and Stephen J. Redding, eds., *Handbook of Regional and Urban Economics*, Vol. 6, Elsevier, 2025, pp. 73–141.

_ , "Spatial Economics," *Oxford Research Encyclopedia of Economics and Finance*, 2025.

_ **and Daniel Sturm**, "The cost of remoteness: Evidence from German division and reunification," *American Economic Review*, 2008, *98* (5), 1766–1797.

_ **and Esteban Rossi-Hansberg**, "Quantitative spatial economics," *Annual Review of Economics*, 2017, *9*, 21–58.

Sandholm, William H., *Population Games and Evolutionary Dynamics*, MIT Press, 2010.

Smith, Michael J., "The stability of a dynamic model of traffic assignment: An application of a method of Lyapunov," *Transportation Science*, 1984, *18* (3), 245–252.

Sugimoto, Tatsuya, Yuki Takayama, and Akiyoshi Takagi, "A quantitative spatial model for evaluating transport-induced spatial reorganization," *Transport Policy*, 2025, *172*, 103738.

Tabuchi, Takatoshi, "Urban agglomeration and dispersion: A synthesis of Alonso and Krugman," *Journal of Urban Economics*, 1998, *44* (3), 333–351.

_ **and Jacques-François Thisse**, "A new economic geography model of central places," *Journal of Urban Economics*, 2011, *69* (2), 240–252.

_ **and Jacques-François Thisse**, "Taste heterogeneity, labor mobility and economic geography," *Journal of Development Economics*, 2002, *69* (1), 155–177.

Takayama, Yuki and Takashi Akamatsu, "Emergence of polycentric urban configurations from combination of communication externality and spatial competition (in Japanese)," *Journal of JSCE Series D3: Infrastructure Planning and Management*, 2011, *67* (1), 1–20.

_ **, Kiyohiro Ikeda, and Jacques-François Thisse**, "Stability and sustainability of urban systems under commuting and transportation costs," *Regional Science and Urban Economics*, 2020, *84*, 103553.

Taylor, Peter D. and Leo B. Jonker, "Evolutionarily stable strategies and game dynamics," *Mathematical Biosciences*, 1978, *40*, 145–156.

Waddell, Paul, "UrbanSim: Modeling urban development for land use, transportation, and environmental planning," *Journal of the American Planning Association*, 2002, *68* (3), 297–314.